

中国激光

新能源汽车用铝合金激光-电弧复合焊接研究进展(特邀)

王晓南^{1,2*}, 陈夏明^{1,2}, 环鹏程³, 李响⁴, 董其鹏^{1,2}, 骆顺存^{1,2}, 长海博文^{1,2}

¹苏州大学沙钢钢铁学院, 江苏 苏州 215021;

²江苏省新能源汽车用金属结构材料绿色制备与资源再生工程研究中心, 江苏 苏州 215021;

³东北大学轧制技术及连轧自动化国家重点实验室, 辽宁 沈阳 110819;

⁴无锡锐科光纤激光技术有限责任公司, 江苏 无锡 214000

摘要 发展新能源汽车是我国从汽车大国迈向汽车强国的必由之路, 是应对气候变化、推动绿色发展的战略举措。近年来, 作为新能源汽车制造的重要结构材料, 车用铝合金性能的不断提升给后续的焊接加工带来了全新的挑战。与传统弧焊热源相比, 激光-电弧复合热源具有诸多优势, 为抑制铝合金焊接缺陷并提升焊接接头系数提供了新途径。较为全面地总结了近年来国内外学者在铝合金焊接缺陷(如软化、气孔)等形成及调控方面的研究进展, 分析了现有研究工作中存在的问题并给出了激光-电弧复合焊接铝合金未来的研究方向, 旨在为后续研究及应用提供参考。

关键词 激光技术; 激光-电弧复合焊接; 铝合金; 软化; 气孔; 力学性能

中图分类号 TG47 文献标志码 A

DOI: 10.3788/CJL231337

1 引言

铝合金因具有低密度、优异的力学性能及耐腐蚀性能等优点, 成为当今汽车行业尤其是新能源汽车行业降低车身自重、提高燃油效率的首选轻质材料^[1-2]。在车身与零部件的生产制造过程中, 不可避免需要考虑到连接问题, 因而如何实现车用铝合金的高效优质连接对车身制造具有重要意义。在综合考虑生产成本、连接效率及质量的因素下, 以熔化极惰性气体保护焊(MIG 焊)^[3]、非熔化极惰性气体钨极保护焊(TIG 焊)^[4-5]及激光焊接^[6]为主的熔化焊工艺已成为车用铝合金的主要连接方式。

为获得优异的强韧性提高汽车身安全性, 铝合金需经大塑性变形、热处理、微合金化等工艺处理以获得精细组织、纳米析出相^[7-9]。然而, 上述组织均具有高温不稳定性, 导致其在焊接热源作用下难以保留。同时, 因铝合金的热膨胀系数与热导系数是钢铁材料的数倍, 获得全熔透焊接接头所需的热输入显著提高, 会进一步加剧焊接热源对上述组织的损伤。因此, 若采用与钢铁材料相匹配的 MIG 焊、TIG 焊等弧焊工艺对车用铝合金进行焊接, 焊接接头尤其是热影响区存在明显软化, 使得软化程度可达到 50%, 从而导致焊接接头系数低于产业化应用需求(70%)。为解决该问题, 国内外研究学者采用高能量密度的激光热源代替

传统弧焊热源, 从而显著降低了焊接热输入, 因而热影响区软化程度降低至 25%~30%。但铝合金作为高反材料, 对激光的吸收率不足 5%, 导致能量利用率低且易造成非必要的激光反射伤害。同时, 为获得较高的能量密度, 激光光斑直径一般为 0.2~0.6 mm, 因而激光焊接对间隙的容忍度较低^[15-16]。此外, 因无焊丝填充, 焊缝存在咬边、凹陷及软化等缺陷。由此可见, 仅采用激光焊接无法满足车用铝合金的产业化焊接需求。

为解决车用铝合金激光焊接存在的问题, 研究学者尝试引入电弧与激光进行耦合, 开发出激光-电弧复合焊接工艺^[17-18], 如图 1 所示。研究指出, 电弧与激光

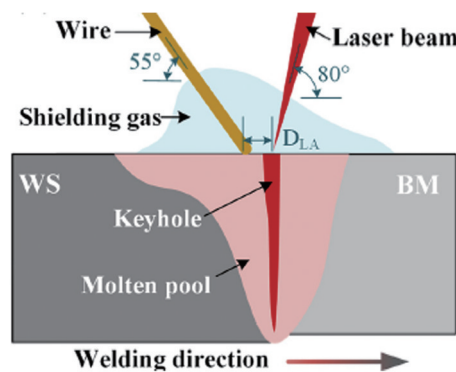


图 1 激光-电弧复合焊接示意图^[17-18]

Fig. 1 Diagram of laser-arc hybrid welding process^[17-18]

收稿日期: 2023-10-30; 修回日期: 2023-11-23; 录用日期: 2023-12-13; 网络首发日期: 2023-12-22

基金项目: 国家自然科学基金面上项目(U1864209)、江苏省“青蓝工程”基金

通信作者: *wxxn@suda.edu.cn

之间的协同效应提高了对激光的吸收率,起到“ $1+1>2$ ”的效果^[19-20]。同时,电弧的引入可提高焊缝成形质量并强化焊缝^[21-24],从而显著提高了车用铝合金焊接接头系数和良品率,更适用于产业化生产。但是不同于单一热源,激光-电弧复合焊接工艺中两种热源的相对位置对焊接稳定性存在明显影响。相比于以电弧在前的电弧引导方式,以激光在前的激光引导方式具有更高的焊接稳定性和对光丝间距的容忍度^[27-29],从而使得其在车用铝合金焊接领域中具有更为广阔的应用前景。此外,为充分发挥该工艺的高效率优势并保证安全性,焊枪角度与试板之间的夹角为 $50^\circ\sim80^\circ$ ^[30-31],激光束与法向方向之间的倾斜角则保持 $5^\circ\sim10^\circ$ ^[32-33],如图1所示。

自Lee等^[34]将激光-电弧复合焊接工艺用于铝合金焊接以来,为推动其在汽车行业的产业化应用,来自中国、意大利及加拿大等国家的众多研究者在铝

合金激光-电弧复合焊接工艺优化及接头组织性能调控方面开展了大量研究。近年来,随着新能源汽车车身铝合金占比的大幅增加,激光器行业的飞速发展与价格的大幅度降低,激光-电弧复合焊接工艺在车用铝合金焊接方面得到了广泛应用。鉴于MIG热源的特性,激光-MIG复合焊接工艺受到了更多研究者的青睐^[35-37](图2)。德国大众汽车已建立车用激光-MIG复合焊接工艺生产线,用于Phaeton车身的全铝车门以及奥迪A8全铝车身关键构件侧顶梁的焊接^[38]。为进一步推动激光-电弧复合工艺在车用铝合金焊接领域中的发展,本文全面总结了近20年来国内外学者在铝合金焊接缺陷(如软化、气孔、裂纹等)形成机理及调控方面的研究进展,分析了现有研究工作中存在的问题,并给出了激光-电弧复合焊接车用铝合金未来的研究方向,旨在为后续研究及应用提供参考。

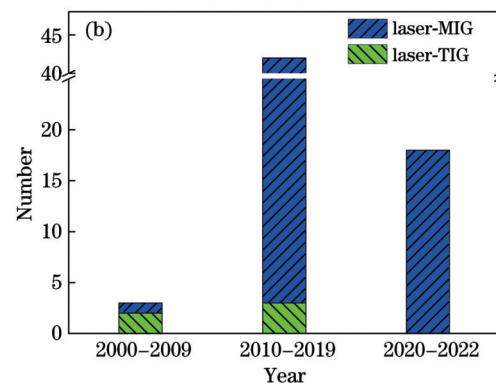
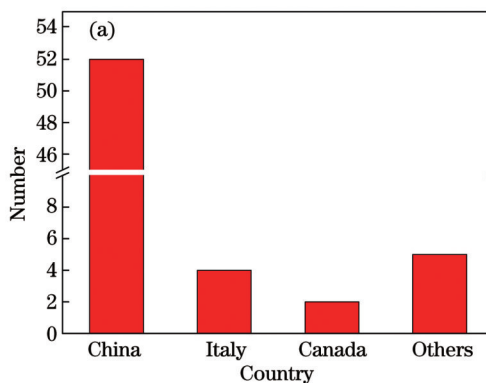


图2 不同分类下的文献统计结果。(a)国家分类;(b)年份分类

Fig. 2 Reference statistical results under different classifications. (a) Countries; (b) years

2 车用铝合金应用现状及焊接难点

2.1 车用铝合金应用现状

根据车身各部位对材料性能要求的不同,在车身制造过程中使用了不同性能的铝合金。以国内新能源汽车领域典型的钢-铝混合车身为例,其采用以挤压与冲压方式生产的包括5xxx、6xxx和7xxx在内的变形铝合金制造车身框架结构件与覆盖件。同时采用以砂模、铁模、熔模与压铸法等方式生产的铸造铝合金制造一体化零部件,如图3所示。不同于车身框架结构件与覆盖件,一体化零部件无需焊接。因此,本文主要关注激光-电弧复合焊接工艺在新能源汽车领域变形铝合金上的应用现状与未来发展方向。

根据强化机制的不同,车用变形铝合金可分为不可热处理和可热处理合金,其中不可热处理合金主要指的是无需热处理的Al-Mg(-Mn)合金(5xxx铝合金)^[39],可热处理铝合金则指的是热处理强化的Al-Mg-Si(-Cu)合金(6xxx铝合金)^[40]和Al-Zn-Mg(-Cu)合金(7xxx铝合金)^[41]。强化机制的不同使得三

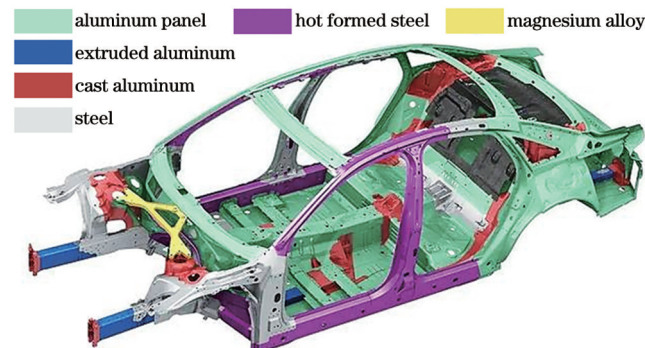


图3 典型新能源汽车多材料钢-铝混合车身

Fig. 3 Multi-material steel-aluminum hybrid body of typical new energy vehicle

种合金的力学性能存在差异,因而所制备的零部件略有不同。

2.1.1 Al-Mg(-Mn)合金

Al-Mg(-Mn)合金借助固溶强化和精细组织获得最佳的力学性能^[42],具有优异的成形性,多用于覆盖件和冲压结构件的制造。常用Al-Mg(-Mn)合金成分如表1所示。

表 1 典型 Al-Mg(-Mn) 合金的化学成分(质量分数, %)
Table 1 Chemical compositions of typical Al-Mg(-Mn) alloys (mass fraction, %)

Alloy	Si	Fe	Cu	Mn	Mg
5052	≤0.25	≤0.40	≤0.10	≤0.10	2.2~2.8
5182	≤0.20	≤0.35	≤0.15	0.20~0.50	4.0~5.0
5754	0.40	≤0.35	0.10	0.50	2.6~3.6

2.1.2 Al-Mg-Si(-Cu)合金

不同于 Al-Mg(-Mn) 合金, Al-Mg-Si(-Cu) 合金中的合金元素含量较低, 主要借助固溶+时效的热处理工艺析出细小纳米析出相, 并借助大塑性变形获得精细组织, 进而获得优异的强塑性^[43]。研究表明

, 因峰值时效时纳米析出相 β'' 相的析出, Al-Mg-Si(-Cu) 合金的屈服强度可达到 200~400 MPa, 多用于副车架、控制臂、防撞梁等车身承力与吸能部件的制造。常用车用 Al-Mg-Si(-Cu) 合金成分如表 2 所示。

表 2 典型 Al-Mg-Si(-Cu) 合金的化学成分(质量分数, %)
Table 2 Chemical compositions of typical Al-Mg-Si(-Cu) alloys (mass fraction, %)

Alloy	Si	Fe	Cu	Mn	Mg
6063	0.2~0.6	<0.35	0.1	0.1	0.45~0.90
6005	0.5~0.9	<0.35	0.3	0.50	0.4~0.7
6009	0.6~1.0	<0.5	0.15~0.60	0.2~0.8	0.4~0.8
6010	0.8~1.2	<0.5	0.15~0.60	0.2~0.8	0.4~0.8
6111	0.7~1.1	<0.40	0.5~0.9	0.15~0.45	0.5~1.0
6022	0.8~1.5	0.05~0.20	0.01~0.10	0.02~0.10	0.45~0.70
6016	1.0~1.5	<0.5	<0.2	<0.2	0.25~0.60
6082	0.7~1.3	0.5	0.1	0.4~1.0	0.6~1.2
6181A	0.7~1.1	0.15~0.50	<0.25	<0.4	0.6~1.0

2.1.3 Al-Zn-Mg(-Cu)合金

不同于 Al-Mg-Si(-Cu) 合金, Al-Zn-Mg(-Cu) 合金中的合金元素含量较高, 并依靠纳米析出相 η'' 和 η' 相的析出^[44], 其屈服强度可达到 300~500 MPa。因此,

Al-Zn-Mg(-Cu) 合金已被视为代替热成形钢制备汽车 B 柱的高强车用铝合金, 主要用于车身承力与吸能部件的制造, 如防撞梁、B 柱及吸能盒等。常用车用 Al-Zn-Mg(-Cu) 合金成分如表 3 所示。

表 3 典型 Al-Zn-Mg(-Cu) 合金的化学成分(质量分数, %)
Table 3 Chemical compositions of typical Al-Zn-Mg(-Cu) alloys (mass fraction, %)

Alloy	Zn	Mg	Cu	Si	Fe	Zr
7003	6.20~6.60	0.68~0.72	0.16~0.20	0.12	0.20	0.15~0.19
7108	4.50~5.50	0.70~1.40	≤0.05	≤0.10	≤0.10	0.12~0.25
7046	6.60~7.60	1.00~1.60	≤0.25	≤0.20	≤0.40	0.10~0.18
7075	5.10~6.10	2.10~2.90	1.20~2.00	0.40	0.50	0.10~0.18

2.2 车用铝合金焊接问题

不同于钢铁材料, 铝合金独特的物理化学特性, 如密度与熔点低、导热系数与热膨胀系数大、活泼性高等, 使得其焊接接头存在软化、气孔及热裂纹的问题, 具体表现如下。

2.2.1 软化

在焊接热源的作用下, 母材中原有的精细组织与纳米析出相无法保留, 使得焊缝与热影响区均存在明显软化, 因而焊接接头的强度较母材显著降低, 如图 4(a)所示。因母材强化机制的不同, 焊接接头软

化程度略有不同。对于以析出强化为主的可热处理铝合金—Al-Mg-Si(-Cu)合金和Al-Zn-Mg(-Cu)合金,焊接接头软化程度可达到40%~50%^[45-46],而对于以固溶强化与细晶强化为主的不可热处理铝合金—Al-Mg(-Mn)合金,焊接接头软化程度则低于30%^[47-48]。此外,焊接接头软化程度还与热输入有关,降低焊接热输入可有效降低焊接接头软化程度^[49]。因此,在研究车用铝合金焊接接头的软化机理的基础上,研究者在车用铝合金激光-电弧复合焊接头软化调控方面展开了广泛的研究,这将在第3节中详细阐述。

2.2.2 气孔

对于铝合金熔焊焊缝而言,因氢在液相和固相中的溶解度差异巨大(相差约20倍)^[50],熔池凝固过程中氢溶解度突降使得残余液相中的氢处于过饱和状态,氢原子依托凝固前沿转变为氢气泡并被凝固前沿捕获而形成氢气孔^[51-52],如图4(b)所示。氢气孔的存在一方面减小了焊缝有效截面积,另一方面应力易在气孔处集中,导致裂纹在气孔处萌生,从而使得焊接接头的静动态力学性能有所降低。除氢气孔外,因激光的引入,激光-电弧复合焊缝中还存在大尺寸的匙孔型气孔,从而显著提高了焊缝气孔倾向。因此,为解决激光-电弧复合焊缝中的高气孔倾向,研究者在匙孔型气孔形成与调控机理方面展开了系统研究,这将在第4节中详细阐述。

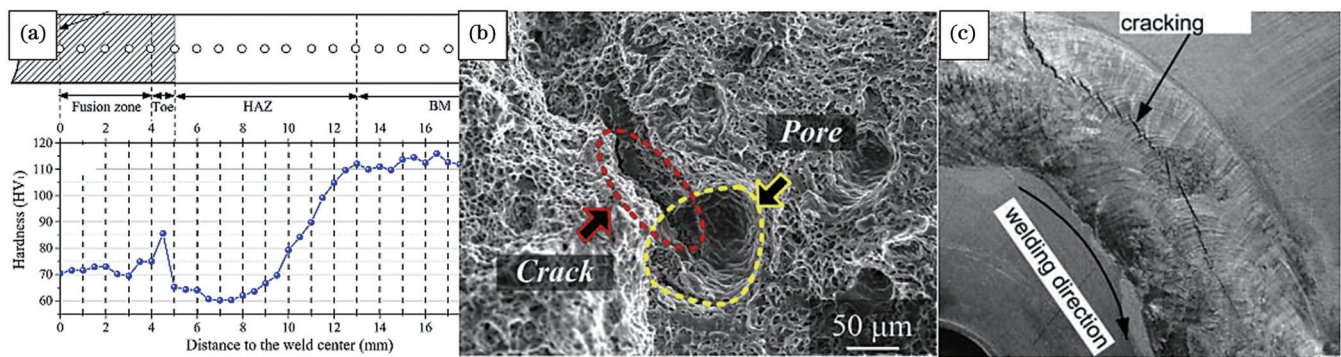


图4 铝合金典型焊接缺陷。(a)接头软化^[45]; (b)气孔^[52]; (c)裂纹^[53]

Fig. 4 Typical welding defects of aluminum alloy. (a) Joint softening^[45]; (b) pore^[52]; (c) crack^[53]

综上所述,解决接头软化与气孔缺陷是实现车用铝合金焊接接头强韧化的关键。因此,研究者对接头软化机理及气孔形成机制展开了广泛的研究,并提出了相应的调控手段,以实现车用铝合金激光-电弧复合焊接接头的强韧化。

3 接头软化形成与调控研究

由2.2小节可知,车用铝合金自身强化机制的不同使得焊接接头的软化程度有所不同,因而焊接接头的软化机理有所不同。本节总结分析了研究者在车用铝合金焊接接头软化机理与调控方面作出的研究与

2.2.3 热裂纹

铝合金较高的热膨胀系数、凝固前后极大的体积变化及含量较高的合金元素,使得焊缝极易形成热裂纹,如图4(c)所示。根据热裂纹形成机理和裂纹位置的不同,铝合金焊接裂纹可分为凝固裂纹和液化裂纹^[53-54]。凝固裂纹多存在于焊缝中心及焊缝终止焊坑内,而液化裂纹主要存在于部分熔化区。为抑制焊缝热裂纹的形成,研究者深入研究了其形成机理。研究指出,在铝合金凝固末期,因晶间结合力降低,在焊接拉应力的作用下晶间液膜开裂形成热裂纹^[55]。同时,大量研究指出,当固相率接近1时,凝固曲线的陡度($dT/df_s^{1/2}$,其中T为温度, f_s 为固相分数)越大,即热裂纹敏感指数(CSI)越大,热裂纹倾向越高^[56]。因而,即使在低残余应力的铝合金激光焊缝中,由于存在较高的温度梯度,裂纹敏感指数处于高位水平,故易形成热裂纹^[55]。为抑制激光焊缝中的热裂纹,研究者从填充焊丝着手,调控熔池凝固行为,降低焊缝的热裂纹敏感指数^[55]。但不同于激光焊或激光填丝焊,激光-电弧复合焊接工艺因电弧的引入,熔池中的温度梯度有所降低,因而仅在高溶质含量的Al-Zn-Mg(-Cu)合金和Al-Mg合金中观察到少量热裂纹^[57-58]。同时研究指出,通过预热与焊丝成分优选等方法降低残余应力或调控焊缝凝固行为,已基本解决焊缝热裂纹问题^[58-59]。因此,在后续研究中将不再叙述关于焊缝凝固裂纹调控方面的研究。

贡献。

3.1 接头软化机理

3.1.1 可热处理铝合金

由2.1小节可知,对于车用可热处理铝合金Al-Mg-Si(-Cu)合金和Al-Zn-Mg(-Cu)合金而言,其主要利用热处理工艺促使纳米析出相的析出,如 β'' 、 η'' 、 η' 相等,以获得优异的力学性能。然而,该类型纳米析出相均为亚稳相,具有热力学不稳定性,因而在高温作用下易发生形态和结构的转变^[10, 60],从而导致其析出强化作用被削弱。因此,车用可热处理铝合金的热影响区软化不仅与晶粒粗化有关,还与纳米析出相的演变

规律有关。

为揭示可热处理铝合金的热影响区软化与纳米析出相演变规律的本质联系,Ambriz 等^[61]基于焊接热循环的峰值温度对纳米析出相演变规律的影响,将热影响区细分为过时效区、淬火区与部分熔化区,如图 5(a)所示。可以看出,过时效区的峰值温度介于母材的时效与固溶温度之间,主要发生纳米析出相的粗化、溶解与转变。在该区域内,随着峰值温度的提高,纳米析出相的粗化和溶解程度逐渐提高,并逐步转变为粗大平衡相,如 β'' 相沿其时效顺序 $[\beta'' \rightarrow \beta' \text{, U1}(\text{MgAl}_2\text{Si}_2) \text{, U2}(\text{Mg}_2\text{Al}_2\text{Si}_2) \text{, B}'(\text{Mg}_9\text{Al}_3\text{Si}_7) \rightarrow \beta \text{, Si}]$,逐步转变为平衡相 β 相, η'' 相则沿 $\eta'' \rightarrow \eta' \rightarrow \eta$ 的时效顺序逐步转变为平衡相 η 相。析出强化作用逐步降低直至消失是该区域软化程度最高的主要原因。在 Jin 等^[62-65]的研究中也存在相同的结果。不同于过时效区,淬火区的峰值温度介于母材的固溶温度与固相线之间。该区域内的纳米析出相完全溶解,基体溶质元素的含量有所增加。依靠固溶强化,该区域的软化程度则有所降低。部分熔化区的峰值温度则介于固相线与液相线之间,除存在纳米析出相溶解

外,还存在晶界熔化,导致晶粒粗化并形成沿晶界分布的粗大析出相,从而消耗了部分溶质原子。因此,该区域的软化程度较淬火区有所提高,但仍略低于过时效区。根据纳米析出相的演变规律对热影响区软化程度的影响,典型可热处理铝合金焊接接头的热影响区硬度分布如图 5(c)所示^[66]。

不同于热影响区,焊缝因发生重熔再结晶,组织转变为典型的粗大铸造组织,如图 5(a)所示。由此可见,焊缝软化可归结为两方面:一方面,焊缝粗大铸造组织导致母材变形获得的细小晶粒完全消失;另一方面,因重熔再结晶,焊缝中无纳米级析出相存在,仅存在粗大的亚微米和微米级析出相,从而大幅削弱了析出强化作用。同时,沿晶界和枝晶臂析出的粗大析出相,消耗了大量溶质元素,从而削弱了固溶强化作用^[67-70]。此外,在焊接热源作用下,低熔点的溶质元素如 Zn、Mg 等元素发生烧损^[71]。因此,即使在焊丝填充引入额外溶质元素的条件下,焊缝仍存在明显的软化现象,软化程度可达到 40% 以上,因而焊缝成为车用可热处理铝合金激光-电弧复合焊接接头的薄弱位置,如图 5(c)所示。

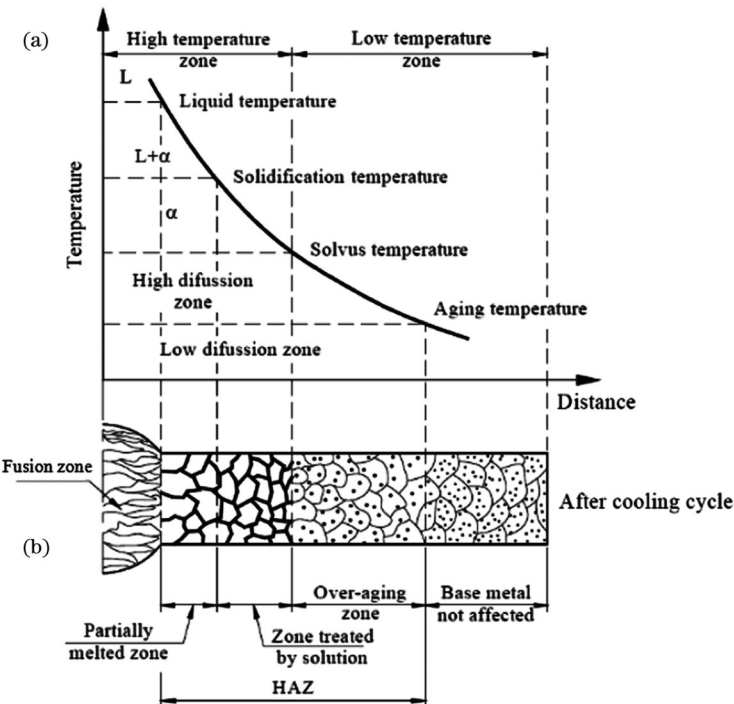


图 5 可热处理合金熔焊接头的显微组织与硬度分布示意图。(a)冷却过程中的焊接热循环^[61]; (b)焊接接头各区域显微组织^[61]; (c)典型激光-电弧复合焊接接头的显微硬度分布^[66];

Fig. 5 Microstructure and hardness distribution of fusion welded joints of heat treatable aluminum alloys. (a) Welding heat cycling during cooling^[61]; (b) microstructure of each area of welded joint^[61]; (c) microhardness distribution of typical laser-arc hybrid welded joints^[66]

不同于车用 Al-Mg-Si(-Cu) 合金,车用 Al-Zn-Mg(-Cu) 合金因含有 0.08%~0.15% (质量分数) 的 Zr 元素,焊缝边部存在由尺寸为几微米等轴晶组成的精细等轴区(FQZ)。FQZ 处的高冷却速度使得溶质元素 Zn、Mg 和 Cu 在晶界处的富集程度明显提高,从而导

致晶界析出大量粗大析出相,如图 6(c)所示。粗大析出相的析出消耗了大量溶质元素,使得焊丝填充所带来的固溶强化作用有所降低,因而 FQZ 成为车用 Al-Zn-Mg(-Cu) 合金激光-电弧复合焊接接头的薄弱位置,如图 6(a)所示^[72]。

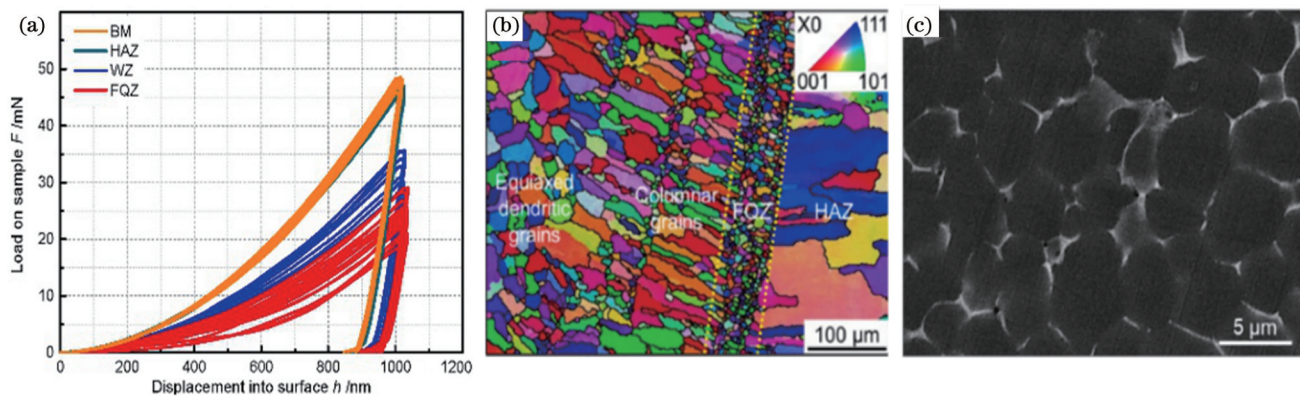


图 6 Al-Zn-Mg-Cu 合金激光-电弧复合焊接接头的组织性能分析结果^[72]。(a) 纳米压痕测试结果; (b) FQZ 晶粒形态; (c) FQZ 显微组织

Fig. 6 Analysis results of microstructure and properties of laser-arc hybrid welded joints of Al-Zn-Mg-Cu alloys^[72]. (a) Nano indentation test results; (b) grain morphology of FQZ; (c) microstructure of FQZ

3.1.2 不可热处理铝合金

不同于可热处理铝合金,不可热处理铝合金主要借助固溶强化和精细组织来获得优异的力学性能。但是,在焊接热源作用下,因晶粒回复、再晶粒及晶粒粗化,母材的精细组织近乎消失,焊缝与热影响区存在明显软化^[73]。此外,车用不可热处理铝合金 Al-Mg (-Mn)合金中的主要溶质元素为低沸点的 Mg 元素,在焊接热源下极易发生烧损,从而降低了 Mg 元素所带来的固溶强化作用。因此,若无焊丝填充,焊缝软化程度高于热影响区。但对于激光-电弧复合焊接工艺而

言,因商用 Al-Mg 系焊丝的填充,Mg 元素烧损所带来的焊缝软化作用得到弥补。对于低 Mg 合金,如 5052、5754 合金,焊丝中约 5% (质量分数) 的 Mg 不仅弥补了烧损的 Mg 元素,还使得焊缝中的 Mg 含量高出母材,从而抵消了晶粒粗化带来的焊缝软化问题,因而焊缝无明显软化,如图 7(a) 所示。但对于高 Mg 合金,如 5183 合金,商用 Al-Mg 系焊丝填充无法弥补 Mg 元素烧损所带来的不利作用,导致焊缝 Mg 含量低于母材和热影响区,因而焊缝软化程度高于热影响区^[47-48],如图 7(b) 所示。

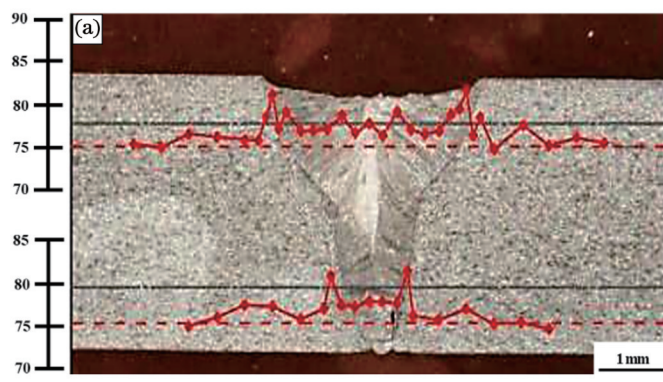


图 7 Al-Mg 合金激光-MIG 复合焊接接头的显微硬度分布。(a) 低 Mg 合金^[48]

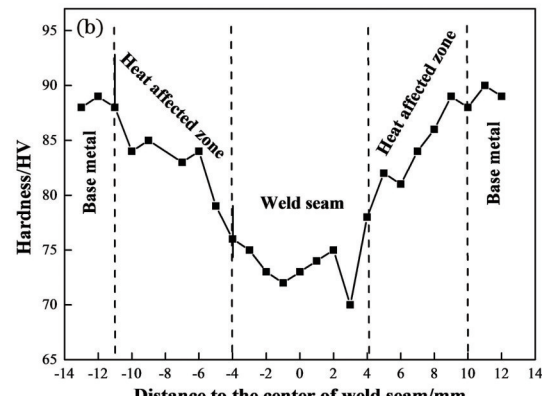
Fig. 7 Microhardness distributions of Al-Mg alloy laser-MIG hybrid welded joints. (a) Low Mg alloy^[48]; (b) high Mg alloy^[47-48]

综上所述,对于车用变形铝合金而言,实现激光-电弧复合焊接接头的强韧化关键在于降低热影响区和焊缝的软化程度,尤其是焊缝软化程度。为此,研究者在焊接接头组织性能调控方面开展了大量研究,以期提高车用铝合金激光-电弧复合焊接接头的力学性能。

3.2 接头软化调控

3.2.1 热影响区软化调控

由上述分析可知,纳米析出相的粗化、回溶及转变是车用可热处理铝合金焊接接头的热影响区存在明显



软化的主要原因。纳米析出相的演变主要与其构成原子的固相扩散速率有关。因此,降低热输入以提高焊接热循环中的加热和冷却速度,将有助于缩短高温停留时间,从而有效抑制原子的扩散,因此可抑制纳米析出相的粗化、溶解及转变。此外,高温停留时间的缩短也可有效抑制再结晶行为,降低车用不可热处理铝合金焊接热影响区的晶粒粗化程度。因此,降低热输入是目前降低热影响区软化程度的主要措施之一。

相比于高能量密度的激光热源,较低能量密度的弧焊热源具有更高的热输入。因此,研究者尝试从弧

焊工艺优化方面降低激光-电弧复合焊接工艺的热输入,进而强化热影响区。21世纪初,在MIG焊接工艺基础上,通过精确控制焊接电流和熔滴过渡过程中的焊丝抽拉行为开发的冷金属过渡(CMT)焊接工艺受到了广泛关注^[74]。相比于MIG焊接工艺,独特的焊丝抽拉行为可使短路过渡中的电流突降至零,从而显著降低其热输入^[75-76]。同时,独特的短路过渡方式实现了稳定、无飞溅的熔滴过渡,有助于提高焊接稳定性^[77]。目前,CMT焊接工艺已被特斯拉、奥迪及蔚来等知名汽车厂商用来制造铝合金车身零部件。

Xin等^[78]采用激光-CMT复合焊接工艺(LCHW)成功实现了Al-Mg-Si合金的优质焊接,焊缝成形良

好,焊接接头的抗拉强度可达到母材的80%以上。在此基础上,Zhang等^[79-80]对比分析了车用Al-Mg-Si合金激光-脉冲MIG复合焊(LPMHW)和LCHW焊接接头的组织性能。研究结果表明,相比于LPMHW焊接接头,CMT焊接工艺的低热输入使得LCHW焊接接头的热影响区的软化程度和宽度分别降低了5%和20%,如图8所示。因而车用Al-Mg-Si合金激光-CMT复合焊接接头的抗拉强度可提高3%~10%,焊接接头系数可达到80%以上。为推广该工艺,奥地利Fronius公司结合车身结构的复杂特性,研发了多款激光-CMT复合焊专用激光头,可实现车身角接、直焊缝的高效优质焊接^[81]。

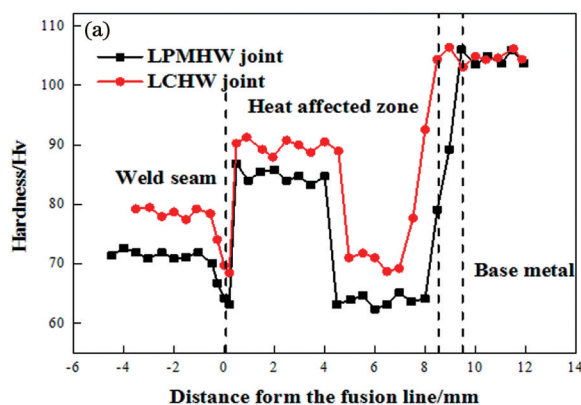


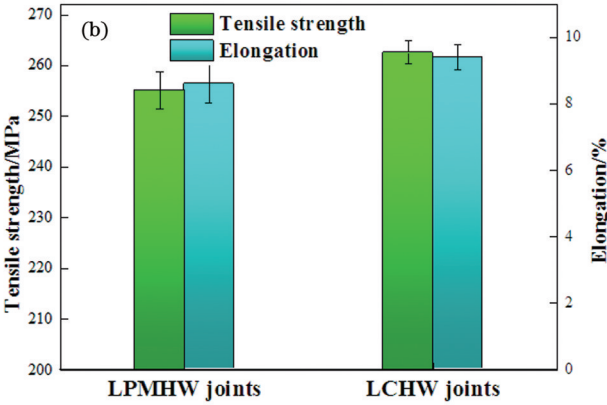
图8 车用Al-Mg-Si合金激光-电弧复合焊接接头的力学性能^[80]。(a)显微硬度分布;

Fig. 8 Mechanical properties of laser-arc hybrid welded joints of Al-Mg-Si alloys for vehicle use^[80]. (a) Microhardness distribution; (b) mechanical properties

3.2.2 焊缝软化调控

3.2.2.1 基于焊丝体系优选的焊缝软化调控研究

由3.1小节可知,对于激光-电弧复合焊焊缝而言,焊丝填充所带来的溶质元素补充,可提高焊缝的固溶强化作用,从而降低焊缝的软化程度。不同的焊丝体系,所引入的溶质元素种类与强化效果均存在差异^[82]。因此,为解决激光-电弧复合焊焊缝软化问题,研究者尝试从焊丝优化选择方面调控焊缝组织性能。研究结



果表明,相比于常用Al-Mg系焊丝,Al-Si系焊丝使得焊缝中的Mg含量有所降低,但显著提高了焊缝中的Si含量。对比而言,Si原子较大的原子半径使得其固溶强化作用高于Mg原子,如图9(a)所示^[83]。因此,相比于Al-Mg系焊丝,采用Al-Si系焊丝得到的焊缝强度提高了约32%,达到母材的80%以上,如图9(b)所示^[83]。此外,在Yan等^[84]的早期研究中指出,相比于Al-Mg系焊丝,Al-Cu系焊丝也有助于降低焊缝软化

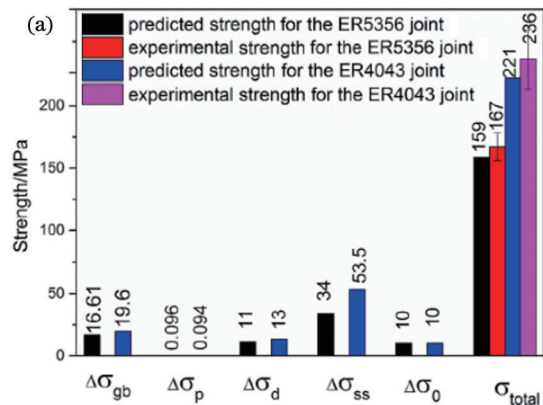
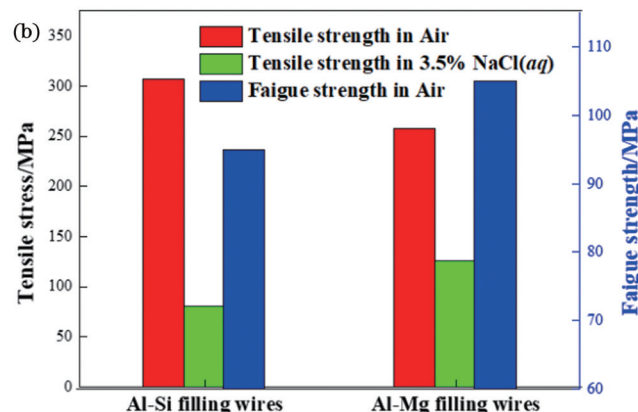


图9 焊丝成分对Al-Mg-Si合金激光-MIG复合焊接接头力学性能的影响^[83]。(a)焊缝强化机制;

Fig. 9 Effects of wire composition on mechanical properties of laser-MIG hybrid welded joints of Al-Mg-Si alloys^[83]. (a) Strengthening mechanism of weld seam; (b) mechanical property



程度。由此可见,通过焊丝优选可有效降低焊缝软化程度,提高车用铝合金激光-电弧复合焊接接头的力学性能。

虽然优选焊丝体系可降低焊缝软化程度,但研究表明,焊丝体系的变化会影响焊缝金属的热物性。本课题组前期的研究结果表明,相比于 Al-Mg 系焊丝,Al-Si 系焊丝提高了熔池凝固速度,从而提高了焊缝中气孔逸出的难度,因而焊缝气孔率明显提高^[85]。较高气孔率使得焊接接头的塑性和疲劳性能显著恶化。此外,Al-Si 共晶组织在腐蚀环境中充当阳极,提高了焊缝的腐蚀倾向,因而对处于临海等含 Cl⁻环境中的车用铝合金焊接接头的服役寿命具有一定的恶化作用^[86]。因此,需根据实际应用环境要求,从多方面综合考虑,优选焊丝体系以强化焊缝。

3.2.2.2 基于熔池对流行为调控的焊缝软化调控研究

由 3.1 小节可知,晶粒粗化是焊缝存在软化的主要原因之一。因此,为细化焊缝晶粒,研究者增强熔池对流,使枝晶破碎,进而提高晶粒形核率,焊缝晶粒尺寸降低 10%。晶粒细化可使焊缝软化程度降低^[87]。为增强熔池对流,外场(磁场或超声场等)辅助受到了关注。但实际生产难以提供足够的空间用于铺设外场。因此,研究者利用摆动激光技术调控熔池对流行为。研究指出,高速移动的光斑可对熔池起到强搅拌作用,从而显著提高熔池对流,因而可有效破碎糊状区优先生成的枝晶尖端,从而抑制柱状晶的生长并促进等轴晶形核,如图 10 所示^[88]。因此,相比于外场辅助,摆动激光技术更符合实际生产工况,正逐步被宁德时代、比亚迪、蔚来等车企用来焊接电池包壳体、车身框架结构及覆盖件。

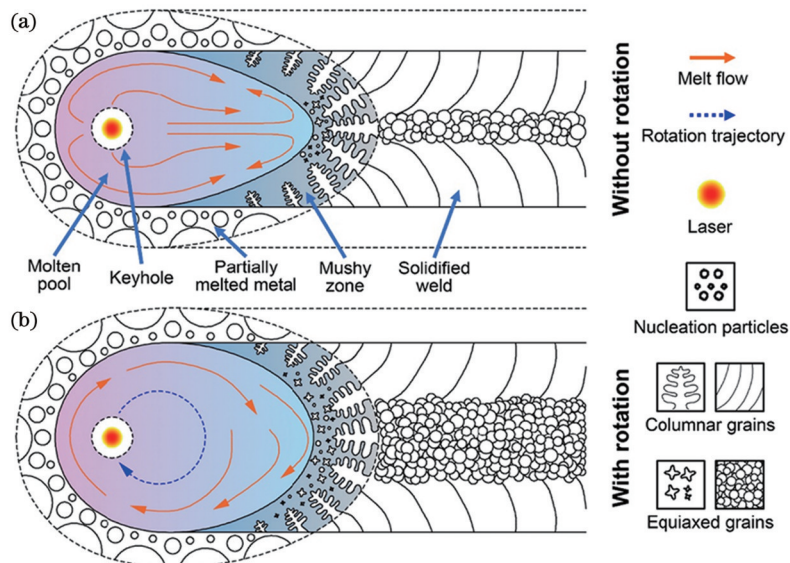


图 10 “O”形摆动激光对焊缝凝固行为的影响^[88]。(a)传统激光焊;(b)“O”形摆动激光焊

Fig. 10 Influence of “O” shaped swing laser on weld solidification behavior^[88]. (a) Traditional laser welding; (b) “O” shape swing laser welding

3.2.2.3 基于焊缝合金化的焊缝软化调控研究

为提高焊缝晶粒细化效果,研究者借用铝合金常用的晶粒细化方法,即焊缝合金化。焊缝合金化使得熔池凝固前析出 Al₃M 相。Al₃M 相作为异质形核点,通过包晶反应 L+Al₃M→α-Al 大幅提高了 α-Al 的形核率,从而抑制了柱状晶的生成。相比于调控熔池对流行为的方法,焊缝合金化方法的细化效果更为明显。通过添加晶粒细化元素,焊缝晶粒尺寸可降低到 10 μm,焊缝强度可提高 5%。

在借助 Al₃M 相细化焊缝晶粒的研究中,Al₃Sc 相受到了广泛关注^[89-90]。Madhusudhan Reddy 等^[91]指出,Sc 合金化可有效细化 Al-Zn-Mg(-Cu) 合金的焊缝晶粒,晶粒尺寸可细化到 20 μm 左右。然而,Sc 元素作为一种稀土元素,造价高昂。为降低成本,Sc-Zr 复合合金化得到了青睐,研究表明,相比于 Sc 合金化,Sc-Zr

复合合金化可提供更多的异质形核点,如 Al₃Sc、Al₃Zr 和 Al₃(Sc_{1-x},Zr_x) 相,也可达到细化晶粒的作用。Yang 等^[92]和 Deng 等^[93]采用 Sr-Zr 复合合金化分别对 Al-Mg 和 Al-Zn-Mg(-Cu) 合金焊缝晶粒尺寸进行调控。研究结果表明,焊缝晶粒尺寸可降低至 10 μm,焊接抗拉强度提高 4%~5%。

虽然复合合金化方法降低了生产成本,但 Sc 元素并不适用于大规模产业化应用,因而目前商业化生产的焊丝仅含有少量的 Zr 元素,如 ER5183 焊丝。为进一步推动焊缝合金化的产业化应用,Wu 等^[94-95]研究了低成本的 Nb 元素对 Al-Zn-Mg(-Cu) 合金激光-电弧复合焊焊接接头组织性能的影响。研究结果指出,Nb 合金化可使 Al₃Nb 相在凝固过程中优先形成并成为异质形核点,从而大幅提高形核率,使得焊缝获得全等轴晶组织。当焊缝中的 Nb 含量(质量分数)达到 0.83% 时,

焊缝晶粒尺寸降低至 $8 \mu\text{m}$, 使得焊缝抗拉强度提高 4%。

实际上, 铝合金中常用的细化剂体系为 Al-Ti-B 系。相比于上述晶粒细化元素, Ti-B 复合合金化细化晶粒的效果优异, 且造价更为低廉。Adisa 等^[96]以 Al-5Ti-B 丝作为填充焊丝对 Al-Zn-Mg(-Cu) 合金进行焊接。研究指出, 由于 Al-5Ti-B 丝的填充, 焊缝晶粒尺寸降低至 $2 \mu\text{m}$, 故焊接接头的抗拉强度和屈服强度分别达到母材的 88% 和 97%。

上述研究结果表明, 熔池对流行为调控与焊缝合金化均可有效细化焊缝晶粒, 焊缝晶粒尺寸可降低至 $10 \mu\text{m}$ 及以下。但是, 晶粒细化所带来的强化效果有限, 焊接接头强度仅提高 4.0%~5.0%。在 Hall-Petch 公式中, 晶粒尺寸与细晶强化增量 ($\Delta\sigma_{gb}$) 之间的关系为

$$\Delta\sigma_{gb} = K \times d^{-1/2}, \quad (1)$$

式中: d 为晶粒尺寸; K 为材料常数。对于铝合金而言, K 仅为 0.14^[20-21], 远低于钢铁材料。因此, 与车用钢铁材料不同, 晶粒尺寸的变化并不会大幅度提高铝合金的屈服强度, 这也是采用晶粒细化元素对焊缝进行合金化处理后焊接接头力学性能未显著提升的本质原因。

3.2.2.4 基于纳米高熔点非金属间化合物的焊缝软化调控研究

除固溶强化与细晶强化外, 利用纳米非金属间化合物的弥散强化也可有效强化铝合金。但因激光的引入, 熔池温度最高可达到 2000°C , 为保证纳米非金属间化合物起到弥散强化的作用, 高熔点非金属间化合物得到了广泛研究。

Sokoluk 等^[97]引入高熔点纳米 TiC 颗粒调控 Al-Zn-Mg(-Cu) 合金焊缝组织。研究结果表明, 纳米 TiC 颗粒的添加使得焊缝晶粒尺寸降低至 $10 \mu\text{m}$ 以下。由于纳米 TiC 颗粒的弥散强化和细晶强化作用, 焊缝软化程度低于热影响区, 故热影响区成为焊接接

头的薄弱位置。在 Fattahi 等^[98-100]的研究中亦有相似的结果。同时, Cheng 等^[101]研究发现, 纳米 TiC-TiB₂ 复合颗粒的添加更有利于焊缝强化。由此可见, 高熔点纳米非金属间化合物通过弥散强化和细晶强化作用, 使得车用铝合金弧焊焊缝的力学性能得到明显提升。然而, 受焊接热源的影响, 高熔点纳米非金属间化合物会不可避免地发生一定的粗化。但相比于常规弧焊焊接技术, 激光-电弧复合焊接工艺的热输入显著降低, 从而提高了熔池凝固冷却速度。这将有助于抑制焊接过程中高熔点纳米非金属间化合物的粗化, 从而有利于高熔点纳米非金属间化合物发挥强化焊缝的作用。但是, 激光-电弧复合焊接熔池的尺寸极小, 熔池对流行为复杂, 如何将高熔点纳米非金属间化合物高效均匀地添加到熔池中仍有待进一步研究。

4 气孔形成与调控研究

4.1 气孔形成机理

除焊缝软化外, 气孔对焊接接头静动态力学性能也存在明显的恶化作用。不同于传统弧焊焊缝, 铝合金激光-电弧复合焊缝中除常见的冶金型气孔, 即氢气孔外, 还存在尺寸可达毫米级的工艺型气孔, 即匙孔型气孔^[102-105], 如图 11 所示。相比于氢气孔, 锤孔型气孔不规则的形状和较大的尺寸特征易产生较明显的应力集中现象, 且裂纹倾向于在不规则的气孔尖端处出现, 从而显著降低焊缝的强韧性。Yan 等^[106]研究了 Al-Mg-Si 合金激光-电弧复合焊接接头的组织性能, 指出锤孔型气孔的存在显著提高了焊缝气孔率, 致使焊接接头的抗拉强度降低至 206 MPa , 焊接接头系数不足 80%。此外, Han 等^[107]指出, 因锤孔型气孔的存在, Al-Mg-Si 合金激光-MIG 复合焊接接头的疲劳强度仅为 56 MPa , 低于传统弧焊焊接接头。由此可见, 抑制锤孔型气孔的形成是提高车用铝合金激光-电弧复合焊接接头静动态力学性能的关键。

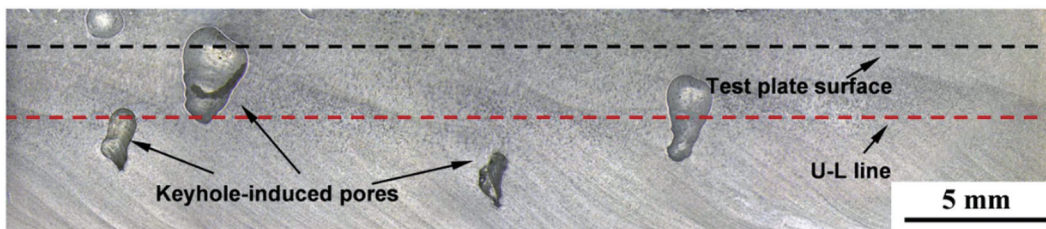


图 11 Al-Mg-Si 合金激光-电弧复合焊缝典型的锤孔型气孔形貌^[105]

Fig. 11 Typical keyhole pore morphology in laser-arc hybrid welds of Al-Mg-Si alloys^[105]

为抑制锤孔型气孔的形成, 首先须明晰其形成机制。Yu 等^[108-110]研究认为, 锤孔型气孔的形成与锤孔稳定性有关。为证明该推论, Wang 等^[111]利用“三明治”结构对 Al-Mg-Si 合金激光电弧焊接过程中的锤孔动态行为进行观察, 结果如图 12 所示。研究结果表明, 当金属蒸气射流作用于锤孔底部时 ($t=1.57 \text{ ms}$),

锤孔前后壁局部区域膨胀并隆起, 导致锤孔发生明显颈缩。此时, 液态金属被局部颈缩的锤孔堵塞, 致使锤孔底部闭合并形成空腔。随着锤孔向前移动, 液态金属无法回填空腔, 最终在焊缝底部形成孔洞缺陷, 如图 12(c) 所示。此外, 当金属蒸气射流作用于锁孔中部时, 锁孔后壁局部隆起并形成气腔。随着锤孔向前

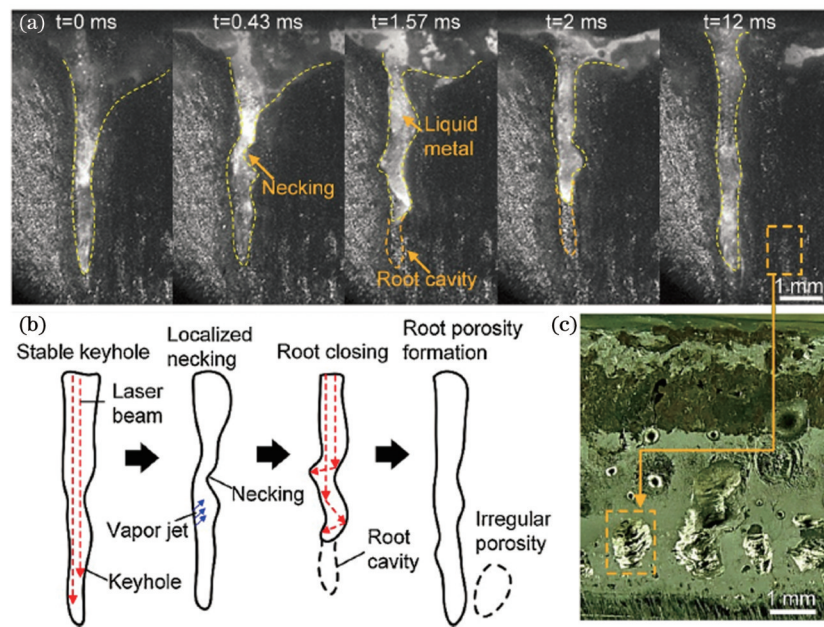


图 12 钥孔型气孔的形成机理示意图^[111]。(a) 钥孔动态行为; (b) 气孔形成示意图; (c) 焊缝剖面图

Fig. 12 Mechanism of keyhole pore formation^[111]. (a) Keyhole dynamic behavior; (b) schematic of pore formation; (c) profile photograph of weld

移动, 气腔转变为气泡, 随后进入熔池并随熔体流向后方。由于激光所形成的熔池尺寸较小, 气泡在上浮过程中易被凝固前沿捕获而形成圆形匙孔型气孔, 气孔多位于焊缝中部和上部, 如图 12(c)所示。由此可见, 提高匙孔稳定性进而抑制匙孔闭合是从根本上消除匙孔型气孔的关键。

4.2 气孔调控

4.2.1 基于摆动激光的气孔调控研究

进入 21 世纪以来, 摆动激光技术被用于提高匙孔

稳定性, 抑制匙孔型气孔的生成。Wang 等^[112]利用摆动激光将铝合金焊缝气孔率降低到 2.5% 以下。Fetzer 等^[113]研究指出, 采用高频($f=200$ Hz)摆动激光可消除铝合金焊缝中的匙孔型气孔。实质上, 摆动激光技术是在常规激光技术的基础上, 利用伺服电机快速摆动激光束偏转镜片, 使得激光束以一定形状的轨迹高速移动, 如图 13(a)所示。根据激光束扫过的轨迹, 可将摆动激光分为“ I ”“ $-$ ”“ O ”和“ ∞ ”形^[114-117]摆动激光。在相同参数下, “ O ”形摆动激光更有利子提高

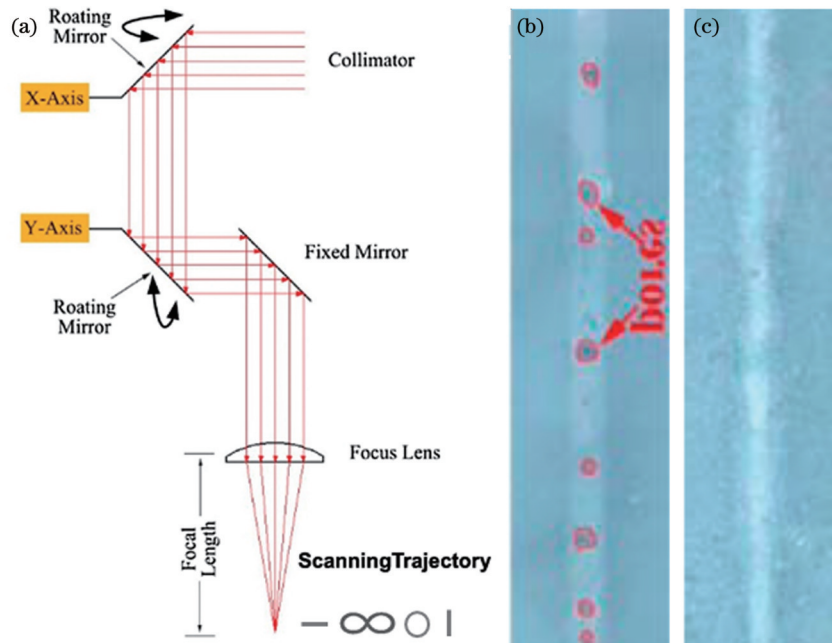


图 13 摆动激光原理及其对焊缝气孔的影响^[113-114]。(a) 摆动激光技术原理图; (b) 激光-电弧复合焊焊缝; (c) 摆动激光-电弧复合焊焊缝

Fig. 13 Principle of swing laser and its effect on weld pore^[113-114]. (a) Schematic of swing laser technology; (b) laser-arc hybrid weld

seam; (c) swing laser-arc hybrid weld seam

匙孔稳定性, 其抑制匙孔型气孔的效果更为优异^[118-119]。因此, 研究者以摆动激光代替传统激光开发出了摆动激光-电弧复合焊接工艺^[120-122], 用于抑制焊缝中匙孔型气孔的形成并取得了优异的抑制效果, 如图 13(c)所示。

大量实验研究表明, 摆动激光抑制匙孔型气孔的效果主要与摆动激光频率和振幅有关。因此, 为建立摆动激光参数与焊缝气孔率之间的本质关系, 同时揭示摆动激光抑制匙孔型气孔的机制, Wang

等^[111]通过三明治结构系统研究了不同摆动参数下匙孔动态行为与焊缝气孔分布之间的关系。研究结果表明, 提高频率和振幅均可大幅提高匙孔运动速度。高速运动的匙孔, 一方面, 扩大了匙孔开口尺寸, 降低了匙孔内的金属蒸气对匙孔后壁的不利影响, 如图 14(a)、(b)所示; 另一方面, 促进了液态金属回填, 降低了匙孔闭合的可能性。因此, 在摆动激光作用下, 钥匙孔稳定性得到提高, 钥匙孔型气孔得到抑制, 如图 14(c)所示。

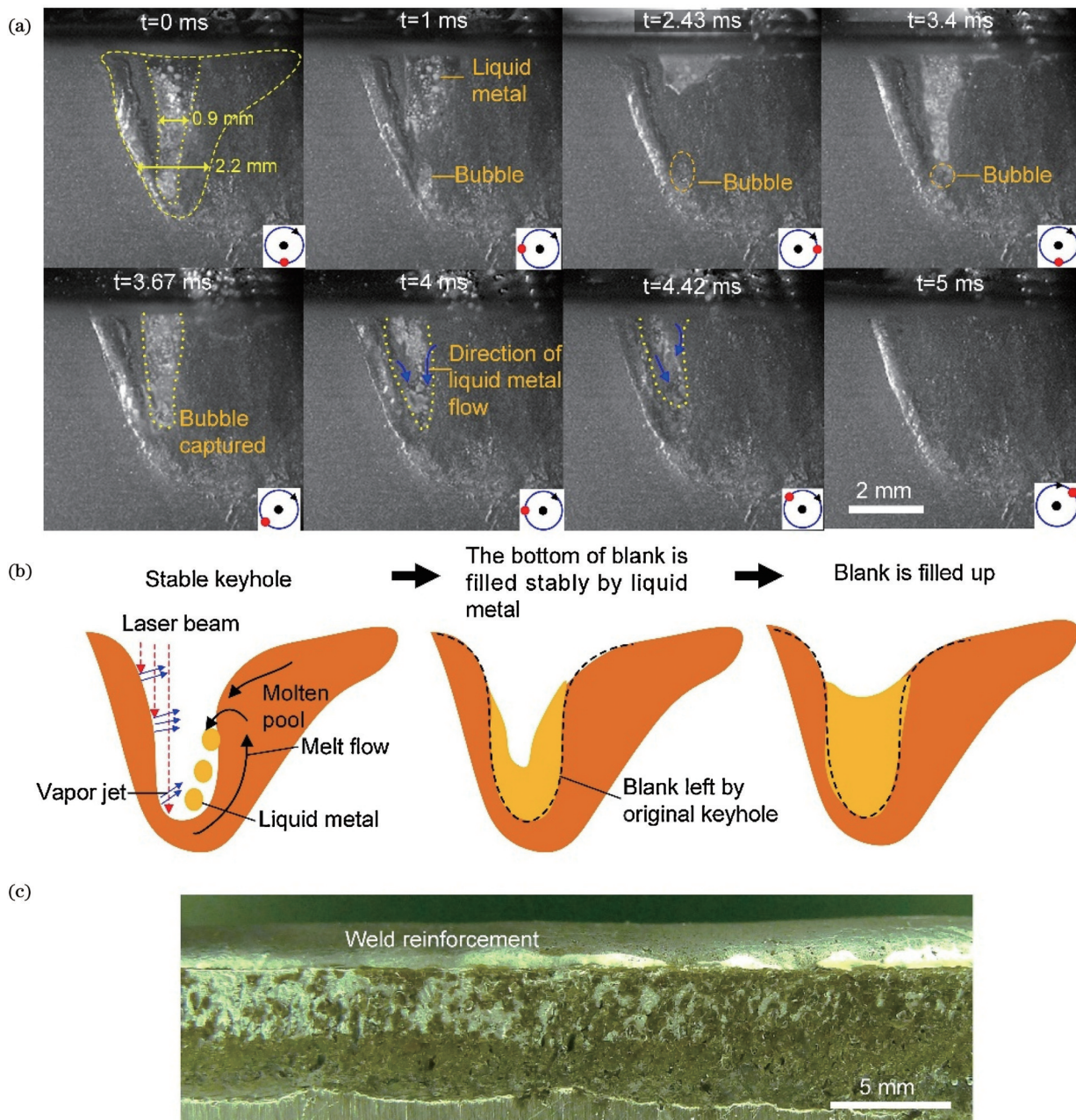


图 14 高振幅高频下匙孔型气孔的抑制机制^[104]。(a)匙孔动态高速摄像结果;(b)熔体填补空腔的过程;(c)焊缝剖面图
Fig. 14 Suppression mechanism of keyhole pore at high oscillating amplitude and high frequency^[104]. (a) High-speed images of keyhole dynamics; (b) process of melt filling cavity; (c) profile photograph of weld

4.2.2 基于焊接工艺的气孔调控研究

在激光-电弧复合焊接工艺中, 熔滴对熔池表面的冲击作用对匙孔后壁形成挤压, 会加剧匙孔闭

合^[123-124]。因此, 研究者尝试通过调控熔滴过渡行为提高匙孔稳定性。研究结果指出, 相比于射滴过渡和射流过渡, 短路过渡通过焊丝抽拉实现熔点过渡, 从而降

低熔滴对匙孔后壁的挤压作用,进而提高匙孔稳定性^[125-127]。因此,相比于其他复合焊接工艺,激光-CMT 复合焊缝中的气孔率较低。

本质上,气孔是熔池凝固过程中气泡被凝固熔池前沿捕获所形成的,因此采用提高热输入的方式,如增大焊接电流和激光功率及降低焊接速度,延长熔池停留时间,从而有效促进气泡的逸出,进而降低焊缝气孔率^[128-130]。Zhang 等^[131]研究了焊接电流、激光功率和焊接速度对 Al-Mg-Si 合金激光-电弧复合焊焊缝形貌及气孔率的影响,建立了焊缝尺寸与焊缝气孔率的关系,为实际生产中通过焊缝尺寸调控降低焊缝气孔率奠定了理论基础。

4.2.3 基于外场辅助的气孔调控研究

对于激光-电弧复合焊接而言,熔滴、电弧及等离子体均含有大量带电粒子,因而在磁场作用下,电弧形状、熔滴过渡行为及等离子体形态均存在明显变化,从而对熔池流动行为产生一定影响^[132]。Tse 等^[133]研究指出,在磁场作用下,等离子体对激光的屏蔽作用减弱,熔深增加约 7%。此外,Li 等^[134]研究指出,磁场可提高匙孔稳定性,减少飞溅,有助于改善焊缝成形。Chen 等^[135]研究了定向磁场辅助对厚板铝合金激光焊接的影响。研究结果表明,水平定向磁场通过诱导额外的涡流形成有限的哈特曼效应,而垂直于表面的磁场则可明显降低熔体流动速度及 Marangoni 对流强度,从而促使熔池温度分布更加均匀,进而改善焊缝成形。此外,在 Zhu 等^[136]的研究中指出,相比于定向磁场,交变磁场在调控熔滴、电弧形态方面的效果更为明显。同时,带电粒子在激光和磁场的共同作用下聚集到一侧,在一定条件下电弧沿焊接方向振荡,从而显著增强熔池对流,进而降低焊缝气孔率。Liu 等^[137]研究发现,磁场波形的变化对等离子体、熔体的流动行为和匙孔的稳定性均存在明显影响。相比于恒定磁场,正弦波交变磁场在增强熔池搅拌作用和提高匙孔稳定性方面效果更佳,焊缝气孔率得到大幅降低。

5 分析与总结

通过热输入调控解决了车用铝合金激光-电弧复合焊接接头热影响区的软化问题,并借助熔滴过渡行为、熔池对流行为、熔池凝固行为及匙孔稳定性调控抑制了匙孔型气孔的形成,从而使得热影响区强度与焊缝气孔率达到产业化应用要求。但是,因车用铝合金多为薄板(厚度≤3 mm),焊丝填充量少,即使通过多种手段增强固溶强化、细晶强化及弥散强化作用,焊缝仍存在明显软化,故焊缝是焊接接头的薄弱位置。而相比于热影响区,焊缝因经历重熔再结晶,呈铸造组织特征,其强韧性较热影响区显著降低,因而车用铝合金尤其是低合金化的车用 Al-Mg-Si 合金的激光-电弧复合焊接接头系数仍低于产业化应用要求(70%)。由此可见,焊缝软化仍是制约激光-电弧复合焊接工艺在新

能源汽车用铝合金焊接领域中进一步推广的主要因素,急需开发适用于激光-电弧复合焊接工艺的新型高性能焊丝。

5.1 低成本高性能焊接材料的设计与开发

已有研究结果表明,现有商用焊丝无法充分发挥激光-电弧复合焊接技术在车用铝合金焊接方面的优势,需对现有焊丝成分进行优化以进一步降低焊缝软化程度。Sc、Zr、Nb 和 Ti-B 微合金化可起到细化晶粒、提高焊缝强度的作用。此外,部分研究者认为,通过添加高熔点纳米级 TiC 可细化晶粒,借助其弥散强化作用可进一步强化焊缝。但就目前而言,有多种元素和颗粒可通过合金化方法提高铝合金的强度,如 Ni 元素^[138]、Mo 元素^[139]、纳米石墨烯^[140]、纳米 SiC^[141]、B₄C 颗粒^[142]及纳米 Al₂O₃ 颗粒^[143]等。因此,还需进一步探究各元素与纳米颗粒对车用铝合金激光-电弧复合焊缝组织性能的影响,以开发出一种或多种可充分发挥激光-电弧复合焊接技术低热输入优势的焊丝。同时通过分析其经济性,以更低的成本实现车用铝合金的优质高性能焊接。此外,单一元素或纳米颗粒无法高效解决焊缝软化问题,采用多组元对焊缝进行合金化处理势在必行。因此,相比于实心焊丝,具有短流程生产、成分柔性化设计特点的药芯焊丝^[144-145]更适用于新型低成本高性能焊接材料的生产,同时也是未来车用铝合金激光-电弧复合焊用新型高性能焊丝的发展方向。

5.2 基于新型激光的复合焊接工艺研究与应用

除上述摆动激光技术外,近期研究者采用由波长不同的半导体激光和光纤激光耦合形成的复合激光热源对铝合金进行焊接。半导体激光波长为 800~1000 nm,铝合金对其的吸收率最高可达到 13%,高于铝合金对光纤激发光的吸收率^[146]。光纤激光焊接基于深熔焊模式,会形成剧烈流动的熔池;而半导体激光焊接基于热传导模式,会形成稳定的熔池,并且易于控制焊缝熔深。因此,复合热源相比于单纯光纤激光具有更高的焊接稳定性。此外,通过调控半导体和光纤激光热源的功率参数可显著提高匙孔稳定性,抑制匙孔型气孔的形成^[147-148]。除半导体激光外,蓝光激光波长更短,铝合金对其的吸收率更高,因而蓝光-光纤复合激光热源在焊接铝合金方面更具优势^[149]。由此可见,基于新型复合激光热源与弧焊热源耦合的新型激光-电弧复合焊接技术将有望进一步实现车用铝合金的高效优质焊接。然而,因复合激光热源的引入,设置复合激光热源与弧焊热源的参数,调控焊缝显微组织和气孔,实现 1+1>2 的效果,是进一步推动新型激光-电弧复合焊接技术应用于车用铝合金焊接领域的关键。同时,新型激光-电弧复合工艺与药芯焊丝之间的相互作用机制对熔滴过渡行为、熔池稳定性、匙孔稳定性、焊接稳定性及焊缝气孔、组织和力学性能的影响亦有待进一步揭示。

参考文献

- [1] Panigrahi S K, Jayaganthan R. A study on the mechanical properties of cryorolled Al-Mg-Si alloy[J]. Materials Science and Engineering: A, 2008, 480(1/2): 299-305.
- [2] Zeng F L, Wei Z L, Li J F, et al. Corrosion mechanism associated with Mg₂Si and Si particles in Al-Mg-Si alloys[J]. Transactions of Nonferrous Metals Society of China, 2011, 21(12): 2559-2567.
- [3] Lin S, Deng Y L, Tang J G, et al. Microstructures and fatigue behavior of metal-inert-gas-welded joints for extruded Al-Mg-Si alloy[J]. Materials Science and Engineering: A, 2019, 745: 63-73.
- [4] Kumar A, Sundarraj S. Effect of welding parameters on mechanical properties and optimization of pulsed TIG welding of Al-Mg-Si alloy[J]. The International Journal of Advanced Manufacturing Technology, 2009, 42(1): 118-125.
- [5] Wang J, Feng J C, Wang Y X. Microstructure of Al-Mg dissimilar weld made by cold metal transfer MIG welding[J]. Materials Science and Technology, 2008, 24(7): 827-831.
- [6] 郭骥之, 王建峰, 郝璐静, 等. 2219铝合金激光镜像焊接接头组织差异性与力学性能研究[J]. 中国激光, 2023, 50(16): 1602101. Guo J Z, Wang J F, Hao L J, et al. Microstructure heterogeneity and mechanical properties of laser mirror welded joint of 2219 aluminum alloy[J]. Chinese Journal of Lasers, 2023, 50(16): 1602101.
- [7] Zhang P, Shi K K, Bian J J, et al. Solute cluster evolution during deformation and high strain hardening capability in naturally aged Al-Zn-Mg alloy[J]. Acta Materialia, 2021, 207: 116682.
- [8] Lee S H, Jung J G, Baik S I, et al. Precipitation strengthening in naturally aged Al-Zn-Mg-Cu alloy[J]. Materials Science and Engineering: A, 2021, 803: 140719.
- [9] Esmaeili S, Lloyd D J, Poole W J. Modeling of precipitation hardening for the naturally aged Al-Mg-Si-Cu alloy AA6111[J]. Acta Materialia, 2003, 51(12): 3467-3481.
- [10] Zhang W K, He H, Xu C C, et al. Precipitates dissolution, phase transformation, and re-precipitation-induced hardness variation in 6082-T6 alloy during MIG welding and subsequent baking[J]. JOM, 2019, 71(8): 2711-2720.
- [11] Zhang L, Li X Y, Nie Z R, et al. Comparison of microstructure and mechanical properties of TIG and laser welding joints of a new Al-Zn-Mg-Cu alloy[J]. Materials & Design, 2016, 92: 880-887.
- [12] Enz J, Riekehr S, Venzke V, et al. Fibre laser welding of high-alloyed Al-Zn-Mg-Cu alloys[J]. Journal of Materials Processing Technology, 2016, 237: 155-162.
- [13] Pinto H, Pyzalla A R, Hackl H, et al. A comparative study of microstructure and residual stresses of CMT-, MIG- and laser-hybrid welds[J]. Materials Science Forum, 2006, 524/525: 627-632.
- [14] Xu G X, Wu C S, Ma X Z, et al. Numerical analysis of welding residual stress and distortion in laser+GMAW hybrid welding of aluminum alloy T-joint[J]. Acta Metallurgica Sinica (English Letters), 2013, 26(3): 352-360.
- [15] Franciosa P, Serino A, Al Botros R, et al. Closed-loop gap bridging control for remote laser welding of aluminum components based on first principle energy and mass balance[J]. Journal of Laser Applications, 2019, 31(2): 022416.
- [16] 王瑜, 舒乐时, 耿韶宁, 等. 汽车车身激光焊接技术的现状与发展趋势[J]. 中国激光, 2022, 49(12): 1202004. Wang Y, Shu L S, Geng S N, et al. Status and development trend of laser welding technology for automotive body[J]. Chinese Journal of Lasers, 2022, 49(12): 1202004.
- [17] Qi X N, Di H S, Wang X N, et al. Effect of secondary peak temperature on microstructure and toughness in ICCGHAZ of laser-arc hybrid welded X100 pipeline steel joints[J]. Journal of Materials Research and Technology, 2020, 9(4): 7838-7849.
- [18] Yan J, Gao M, Zeng X Y. Study on microstructure and mechanical properties of 304 stainless steel joints by TIG, laser and laser-TIG hybrid welding[J]. Optics and Lasers in Engineering, 2010, 48(4): 512-517.
- [19] 赵婷, 张新戈. 铝合金激光-电弧复合焊接研究现状与进展[J]. 焊接, 2012(11): 22-26, 69. Zhao T, Zhang X G. Research status and development on laser-arc hybrid welding of aluminum alloy[J]. Welding & Joining, 2012 (11): 22-26, 69.
- [20] 张禄中, 王晓南, 陈夏明, 等. 激光功率对高强 Al-Mg-Si-Cu 合金激光-CMT 复合焊接接头组织性能的影响[J]. 中国激光, 2023, 50(4): 0402013. Zhang L Z, Wang X N, Chen X M, et al. Effect of laser power on microstructure and properties of high strength Al-Mg-Si-Cu alloy laser-CMT hybrid welded joints[J]. Chinese Journal of Lasers, 2023, 50(4): 0402013.
- [21] Lee K D, Park K Y. A study on the process robustness of Nd: YAG laser-MIG hybrid welding of aluminum alloy 6061-T6[C]// International Congress on Applications of Lasers & Electro-Optics, October 14-18, 2018, Jacksonville, Florida, USA. New York: Laser Institute of America, 2003.
- [22] Uchiumi S, Wang J B, Katayama S, et al. Penetration and welding phenomena in YAG laser-MIG hybrid welding of aluminum alloy[C]//International Congress on Applications of Lasers & Electro-Optics, March 23-25, 2010, San Francisco, California, USA. New York: Laser Institute of America, 2004.
- [23] 张亚亮, 刘佳, 石岩, 等. 电流/电压匹配对铝合金激光-电弧复合焊接过程稳定性的影响[J]. 焊接学报, 2018, 39(1): 79-83, 132. Zhang Y L, Liu J, Shi Y, et al. Effect of current/voltage matching on stability of laser-arc hybrid welding process for aluminum alloy [J]. Transactions of the China Welding Institution, 2018, 39(1): 79-83, 132.
- [24] 张德芬, 杨阳, 王同举, 等. 6009铝合金光纤激光-MIG 电弧复合焊和光纤激光焊工艺对比研究[J]. 材料导报, 2015, 29(12): 121-124, 134. Zhang D F, Yang Y, Wang T J, et al. Comparison of fiber laser-MIG arc hybrid and fiber laser welding of 6009 aluminum alloy[J]. Materials Review, 2015, 29(12): 121-124, 134.
- [25] Kah P, Salminen A, Martikainen J. The effect of the relative location of laser beam and arc in different hybrid welding processes [J]. Mechanics, 2010, 83(3): 68-74.
- [26] Zhao L, Sugino T, Arakane G, et al. Influence of welding parameters on distribution of wire feeding elements in CO₂ laser GMA hybrid welding[J]. Science and Technology of Welding and Joining, 2009, 14(5): 457-467.
- [27] Lei Z L, Li B W, Bi J, et al. Influence of the laser thermal effect on the droplet transfer behavior in laser-CMT welding[J]. Optics & Laser Technology, 2019, 120: 105728.
- [28] Bunaziv I, Akselsen O M, Salminen A, et al. Fiber laser-MIG hybrid welding of 5 mm 5083 aluminum alloy[J]. Journal of Materials Processing Technology, 2016, 233: 107-114.
- [29] Huang S A, Yang X Y, Chen H, et al. Effect of droplet transfer on pore formation in laser-pulsed metal inert gas hybrid welding of A7N01P aluminum alloy[J]. Journal of Laser Applications, 2020, 32(1): 012011.
- [30] Zhao Y Q, Zhou X D, Liu T, et al. Investigate on the porosity morphology and formation mechanism in laser-MIG hybrid welded joint for 5A06 aluminum alloy with Y-shaped groove[J]. Journal of Manufacturing Processes, 2020, 57: 847-856.
- [31] 雷正龙, 黎炳蔚, 朱平国, 等. 波长对激光-CMT 复合焊熔滴过渡行为的影响[J]. 中国激光, 2018, 45 (10): 1002006. Lei Z L, Li B W, Zhu P G, et al. Effect of wavelength on droplet transition behaviors in laser-CMT hybrid welding process[J]. Chinese Journal of Lasers, 2018, 45 (10): 1002006.
- [32] Yan S H, Nie Y, Zhu Z T, et al. Characteristics of microstructure and fatigue resistance of hybrid fiber laser-MIG welded Al-Mg alloy joints[J]. Applied Surface Science, 2014, 298: 12-18.
- [33] Zhang C, Gao M, Zeng X Y. Influences of synergy effect between laser and arc on laser-arc hybrid welding of aluminum alloys[J].

- Optics & Laser Technology, 2019, 120: 105766.
- [34] 韩晓辉, 张志毅, 马国龙, 等. 热源角度对 6A01 铝合金激光-MIG 复合焊成形及气孔的影响[J]. 中国激光, 2022, 49(2): 0202020.
- Han X H, Zhang Z Y, Ma G L, et al. Effects of heat source angle on weld formation and porosity defects of laser-MIG hybrid welding of 6A01 aluminum alloy[J]. Chinese Journal of Lasers, 2022, 49(2): 0202020.
- [35] Chen M H, Xu J N, Xin L J, et al. Comparative study on interactions between laser and arc plasma during laser-GTA welding and laser-GMA welding[J]. Optics and Lasers in Engineering, 2016, 85: 1-8.
- Zhang C, Gao M, Jiang M, et al. Effect of weld characteristic on mechanical strength of laser-arc hybrid-welded Al-Mg-Si-Mn aluminum alloy[J]. Metallurgical and Materials Transactions A, 2016, 47(11): 5438-5449.
- [37] Gao Z G, Wu Y X, Huang J. Analysis of weld pool dynamic during stationary laser-MIG hybrid welding[J]. The International Journal of Advanced Manufacturing Technology, 2009, 44(9): 870-879.
- [38] 肖荣诗, 吴世凯. 激光-电弧复合焊接的研究进展[J]. 中国激光, 2008, 35(11): 1680-1685.
- Xiao R S, Wu S K. Progress on laser-arc hybrid welding[J]. Chinese Journal of Lasers, 2008, 35(11): 1680-1685.
- [39] Hirsch J. Recent development in aluminium for automotive applications[J]. Transactions of Nonferrous Metals Society of China, 2014, 24(7): 1995-2002.
- [40] Engler O, Hirsch J. Texture control by thermomechanical processing of AA6XXX Al-Mg-Si sheet alloys for automotive applications: a review[J]. Materials Science and Engineering: A, 2002, 336(1/2): 249-262.
- [41] Liu C H, Feng Z Z, Ma P P, et al. Reversion of natural ageing and restoration of quick bake-hardening response in Al-Zn-Mg-Cu alloy[J]. Journal of Materials Science & Technology, 2021, 95: 88-94.
- [42] Huskins E L, Cao B, Ramesh K T. Strengthening mechanisms in an Al-Mg alloy[J]. Materials Science and Engineering: A, 2010, 527(6): 1292-1298.
- [43] Pogatscher S, Antrekowitsch H, Leitner H, et al. Mechanisms controlling the artificial aging of Al-Mg-Si Alloys[J]. Acta Materialia, 2011, 59(9): 3352-3363.
- [44] Berg L K, Gjønnes J, Hansen V, et al. GP-zones in Al-Zn-Mg alloys and their role in artificial aging[J]. Acta Materialia, 2001, 49(17): 3443-3451.
- [45] Pramod R, Shanmugam N S, Krishnadason C K. Studies on cold metal transfer welding of aluminium alloy 6061-T6 using ER 4043 [J]. Proceedings of the Institution of Mechanical Engineers, Part L: Journal of Materials: Design and Applications, 2020, 234(7): 924-937.
- [46] Guzmán I, Granda E, Vargas B, et al. Tensile and fracture behavior in 6061-T6 and 6061-T4 aluminum alloys welded by pulsed metal transfer GMAW[J]. The International Journal of Advanced Manufacturing Technology, 2019, 103(5): 2553-2562.
- [47] Huang L J, Wu D S, Hua X M, et al. Effect of the welding direction on the microstructural characterization in fiber laser-GMAW hybrid welding of 5083 aluminum alloy[J]. Journal of Manufacturing Processes, 2018, 31: 514-522.
- [48] Casalino G, Campanelli S, Ludovico A D. Hybrid welding of AA5754-H111 alloy using a fiber laser[J]. Advanced Materials Research, 2012, 628:193-198.
- [49] Vargas J A, Torres J E, Pacheco J A, et al. Analysis of heat input effect on the mechanical properties of Al-6061-T6 alloy weld joints [J]. Materials & Design (1980-2015), 2013, 52: 556-564.
- [50] Avedesian M, Baker H. ASM specialty handbook: aluminum and aluminum alloys[M]. New York: ASM International, 1999.
- [51] Zhu C X, Tang X H, He Y, et al. Characteristics and formation mechanism of sidewall pores in NG-GMAW of 5083 Al-alloy[J]. Journal of Materials Processing Technology, 2016, 238: 274-283.
- [52] Zhu C X, Tang X H, He Y, et al. Study on arc characteristics and their influences on weld bead geometry in narrow gap GMAW of 5083 Al-alloy[J]. The International Journal of Advanced Manufacturing Technology, 2017, 90(9): 2513-2525.
- [53] Kou S. Solidification and liquation cracking issues in welding[J]. JOM, 2003, 55(6): 37-42.
- [54] Cao G, Kou S. Predicting and reducing liquation-cracking susceptibility based on temperature vs. fraction solid[J]. Welding Journal-New York, 2006, 85(1): 9.
- [55] Zhao H, White D R, DebRoy T. Current issues and problems in laser welding of automotive aluminium alloys[J]. International Materials Reviews, 1999, 44(6): 238-266.
- [56] Kou S. A criterion for cracking during solidification[J]. Acta Materialia, 2015, 88: 366-374.
- [57] Casalino G, Morello M. Laser-arc combined welding of AA5754 alloy[J]. Materials Letters, 2021, 284: 128946.
- [58] Ma G Y, Luo X Z, Liu D H, et al. 7075 Aluminum alloy welded by laser-TIG hybrid with homogeneous filler wire: Microstructure evaluation and molten pool behavior[J]. Optics & Laser Technology, 2024, 169: 110059.
- [59] Deng A L, Chen H, Zhang Y B, et al. Prediction of the influence of welding metal composition on solidification cracking of laser welded aluminum alloy[J]. Materials Today Communications, 2023, 35: 105556.
- [60] Zhao D D, Zhou L C, Kong Y, et al. Structure and thermodynamics of the key precipitated phases in the Al-Mg-Si alloys from first-principles calculations[J]. Journal of Materials Science, 2011, 46(24): 7839-7849.
- [61] Ambriz R R, Barrera G, García R, et al. Effect of the weld thermal cycles of the modified indirect electric arc on the mechanical properties of the AA6061-T6 alloy[J]. Welding International, 2010, 24(4): 321-328.
- [62] Jin X Y, Song G H, Zheng W G. Laser-arc hybrid welding properties of aluminum alloy 6005A[J]. Applied Mechanics and Materials, 2014, 651/652/653: 50-55.
- [63] Wanjara P, Cao X J. Hybrid laser-arc welding of AA6061-T6 butt joints[J]. Materials Science Forum, 2014, 783/784/785/786: 2833-2838.
- [64] Myhr O R, Grong Ø, Fjær H G, et al. Modelling of the microstructure and strength evolution in Al-Mg-Si alloys during multistage thermal processing[J]. Acta Materialia, 2004, 52(17): 4997-5008.
- [65] Duan C F, Yang S L, Gu J X, et al. Microstructure and ratcheting behavior of 6061 aluminum alloy laser-MIG hybrid welding joint [J]. Materials Research Express, 2019, 6(8): 086534.
- [66] Wang Q Y, Chen H, Zhu Z T, et al. A characterization of microstructure and mechanical properties of A6N01S-T5 aluminum alloy hybrid fiber laser-MIG welded joint[J]. The International Journal of Advanced Manufacturing Technology, 2016, 86(5): 1375-1384.
- [67] Qiao J N, Lu J X, Wu S K. Fatigue cracking characteristics of fiber Laser-VPTIG hybrid butt welded 7N01P-T4 aluminum alloy [J]. International Journal of Fatigue, 2017, 98: 32-40.
- [68] El-Batahgy A M, Klimova-Korsmik O, Akhmetov A, et al. High-power fiber laser welding of high-strength AA7075-T6 aluminum alloy welds for mechanical properties research[J]. Materials, 2021, 14(24): 7498.
- [69] Wang X M, Li B, Li M X, et al. Study of local-zone microstructure, strength and fracture toughness of hybrid laser-metal-inert-gas-welded A7N01 aluminum alloy joint[J]. Materials Science and Engineering: A, 2017, 688: 114-122.
- [70] Liu S, Li J M, Mi G Y, et al. Study on laser-MIG hybrid welding characteristics of A7N01-T6 aluminum alloy[J]. The International Journal of Advanced Manufacturing Technology, 2016, 87(1): 1135-1144.
- [71] Tang G, Chen H, Yang X Y, et al. Effects of different welding process on the electronic temperature of plasma and weld shape

- during laser-MIG hybrid welding of A7N01P-T4 aluminum alloy [J]. *Journal of Laser Applications*, 2018, 30(2): 022002.
- [72] Hu Y N, Wu S C, Shen Z, et al. Fine equiaxed zone induced softening and failure behavior of 7050 aluminum alloy hybrid laser welds[J]. *Materials Science and Engineering: A*, 2021, 821: 141597.
- [73] Chen L, Wang C M, Xiong L D, et al. Microstructural, porosity and mechanical properties of lap joint laser welding for 5182 and 6061 dissimilar aluminum alloys under different place configurations [J]. *Materials & Design*, 2020, 191: 108625.
- [74] Schierl A. The CMT process a revolution in welding technology [J]. *Welding in the World*, 2005, 49(1): 38.
- [75] Furukawa K. New CMT arc welding process-welding of steel to aluminium dissimilar metals and welding of super-thin aluminium sheets[J]. *Welding International*, 2006, 20(6): 440-445.
- [76] 栗忠秀, 温鹏, 张松, 等. 钨微合金化对光纤激光-CMT 复合焊接 A7204P-T4 铝合金接头组织和力学性能的影响[J]. 中国激光, 2020, 47(9): 0902001.
- Li Z X, Wen P, Zhang S, et al. Effects of Nb micro-alloying on microstructure and mechanical properties of A7204P-T4 aluminum alloy joint by fiber laser-CMT hybrid welding[J]. *Chinese Journal of Lasers*, 2020, 47 (9): 0902001.
- [77] Pickin C G, Young K. Evaluation of cold metal transfer (CMT) process for welding aluminium alloy[J]. *Science and Technology of Welding and Joining*, 2006, 11(5): 583-585.
- [78] Xin Z B, Yang Z B, Zhao H, et al. Comparative study on welding characteristics of laser-CMT and plasma-CMT hybrid welded AA6082-T6 aluminum alloy butt joints[J]. *Materials*, 2019, 12 (20): 3300.
- [79] Zhang C, Li G, Gao M, et al. Microstructure and process characterization of laser-cold metal transfer hybrid welding of AA6061 aluminum alloy[J]. *The International Journal of Advanced Manufacturing Technology*, 2013, 68(5): 1253-1260.
- [80] Han X H, Yang Z B, Ma Y, et al. Comparative study of laser-arc hybrid welding for AA6082-T6 aluminum alloy with two different arc modes[J]. *Metals*, 2020, 10(3): 407.
- [81] Fronius in China[EB/OL]. [2023-09-09]. <https://www.fronius.com.cn/product-51.html>.
- [82] Yoon J W, Lee Y S, Lee K D, et al. Effect of filler wire composition on the Nd: YAG laser weldability of 6061 aluminum alloy[J]. *Materials Science Forum*, 2005, 475/476/477/478/479: 2591-2594..
- [83] Yan S H, Xing B B, Zhou H Y, et al. Effect of filling materials on the microstructure and properties of hybrid laser welded Al-Mg-Si alloys joints[J]. *Materials Characterization*, 2018, 144: 205-218.
- [84] Yan J, Zeng X Y, Gao M, et al. Effect of welding wires on microstructure and mechanical properties of 2A12 aluminum alloy in CO₂ laser-MIG hybrid welding[J]. *Applied Surface Science*, 2009, 255(16): 7307-7313.
- [85] Huan P C, Wang X N, Zhang J, et al. Effect of wire composition on microstructure and properties of 6063 aluminium alloy hybrid synchronous pulse CMT welded joints[J]. *Materials Science and Engineering: A*, 2020, 790: 139713.
- [86] 韩金理, 王松, 张德芬, 等. 6009铝合金激光电弧复合焊接头腐蚀性能研究[J]. 材料导报, 2016, 30(S1): 490-493.
- Han J L, Wang S, Zhang D F, et al. Study on corrosion properties of 6009 aluminum alloy joint by laser-arc hybrid welding[J]. *Materials Reports*, 2016, 30(S1): 490-493.
- [87] Kou S. *Welding metallurgy*[M]. New York: John Wiley & Sons, 2003.
- [88] Yang X Y, Chen H, Li M V, et al. Porosity suppressing and grain refining of narrow-gap rotating laser-MIG hybrid welding of 5A06 aluminum alloy[J]. *Journal of Manufacturing Processes*, 2021, 68: 1100-1113.
- [89] Knippling K E, Dunand D C, Seidman D N. Criteria for developing castable, creep-resistant aluminum-based alloys: a review[J]. *International Journal of Materials Research*, 2022, 97(3): 246-265.
- [90] Wang F, Liu Z L, Qiu D, et al. Revisiting the role of peritectics in grain refinement of Al alloys[J]. *Acta Materialia*, 2013, 61(1): 360-370.
- [91] Madhusudhan Reddy G, Mukhopadhyay A K, Sambasiva Rao A. Influence of scandium on weldability of 7010 aluminium alloy[J]. *Science and Technology of Welding and Joining*, 2005, 10(4): 432-441.
- [92] Yang D X, Li X Y, He D Y, et al. Effect of minor Er and Zr on microstructure and mechanical properties of Al-Mg-Mn alloy (5083) welded joints[J]. *Materials Science and Engineering: A*, 2013, 561: 226-231.
- [93] Deng Y, Peng B, Xu G F, et al. Effects of Sc and Zr on mechanical property and microstructure of tungsten inert gas and friction stir welded aerospace high strength Al-Zn-Mg alloys[J]. *Materials Science and Engineering: A*, 2015, 639: 500-513.
- [94] Wu S K, Li Z X, Qi E Y, et al. Impact of Nb on microstructure and properties of oscillating laser-CMT hybrid welding joints of A7204P-T4 aluminium alloy sheets[J]. *Science and Technology of Welding and Joining*, 2021, 26(4): 273-278.
- [95] Wu S K, Wang C, Li Z X, et al. Effect of Nb micro-alloying on microstructure and properties of A7204-T4 aluminum alloy joints with fiber laser-VPTIG hybrid welding[J]. *Welding in the World*, 2020, 64(9): 1459-1469.
- [96] Adisa S B, Loginova I, Khalil A, et al. Effect of laser welding process parameters and filler metals on the weldability and the mechanical properties of AA7020 aluminium alloy[J]. *Journal of Manufacturing and Materials Processing*, 2018, 2(2): 33.
- [97] Sokoluk M, Cao C Z, Pan S H, et al. Nanoparticle-enabled phase control for arc welding of unweldable aluminum alloy 7075[J]. *Nature Communications*, 2019, 10: 98.
- [98] Fattah M, Mohammady M, Sajjadi N, et al. Effect of TiC nanoparticles on the microstructure and mechanical properties of gas tungsten arc welded aluminum joints[J]. *Journal of Materials Processing Technology*, 2015, 217: 21-29.
- [99] Oropenza D, Hofmann D C, Williams K, et al. Welding and additive manufacturing with nanoparticle-enhanced aluminum 7075 wire[J]. *Journal of Alloys and Compounds*, 2020, 834: 154987.
- [100] Murali N, Sokoluk M, Li X C. Study on aluminum alloy joints welded with nano-treated Al-Mg-Mn filler wire[J]. *Materials Letters*, 2021, 283: 128739.
- [101] Cheng Y, Xu J H, Yu L H, et al. Effect of TiC/TiC-TiB₂ on microstructure and mechanical properties of spray formed 7055 aluminum alloy TIG welded joints[J]. *Journal of Materials Research and Technology*, 2021, 15: 1667-1677.
- [102] Zhao Y Q, Zhan X H, Gao Q Y, et al. Research on the microstructure characteristic and tensile property of laser-MIG hybrid welded joint for 5A06 aluminum alloy[J]. *Metals and Materials International*, 2020, 26(3): 346-359.
- [103] Atabaki M M, Yazdian N, Kovacevic R. Partial penetration laser-based welding of aluminum alloy (AA5083-H32)[J]. *Optik*, 2016, 127(16): 6782-6804.
- [104] Miao H B, Yu G, He X L, et al. Comparative study of hybrid laser-MIG leading configuration on porosity in aluminum alloy bead-on-plate welding[J]. *The International Journal of Advanced Manufacturing Technology*, 2017, 91(5): 2681-2688.
- [105] Huang S, Xu L D, Lou M, et al. Keyhole-induced pore formation mechanism in laser-MIG hybrid welding of aluminum alloy based on experiment and multiphase numerical model[J]. *Journal of Materials Processing Technology*, 2023, 314: 117903.
- [106] Yan S H, Chen H, Zhu Z T, et al. Hybrid laser-metal inert gas welding of Al-Mg-Si alloy joints: Microstructure and mechanical properties[J]. *Materials & Design*, 2014, 61: 160-167.
- [107] Han X H, Yang Z B, Ma Y, et al. Porosity distribution and mechanical response of laser-MIG hybrid butt welded 6082-T6 aluminum alloy joint[J]. *Optics & Laser Technology*, 2020, 132: 106511.
- [108] Yu Y C, Wang C M, Hu X Y, et al. Porosity in fiber laser

- formation of 5A06 aluminum alloy[J]. Journal of Mechanical Science and Technology, 2010, 24(5): 1077-1082.
- [109] Xu G X, Li L, Wang H X, et al. Simulation and experimental studies of keyhole induced porosity in laser-MIG hybrid fillet welding of aluminum alloy in the horizontal position[J]. Optics & Laser Technology, 2019, 119: 105667.
- [110] Xu J J, Rong Y M, Huang Y, et al. Keyhole-induced porosity formation during laser welding[J]. Journal of Materials Processing Technology, 2018, 252: 720-727.
- [111] Wang L, Liu Y, Yang C G, et al. Study of porosity suppression in oscillating laser-MIG hybrid welding of AA6082 aluminum alloy [J]. Journal of Materials Processing Technology, 2021, 292: 117053.
- [112] Wang Z M, Oliveira J P, Zeng Z, et al. Laser beam oscillating welding of 5A06 aluminum alloys: Microstructure, porosity and mechanical properties[J]. Optics & Laser Technology, 2019, 111: 58-65.
- [113] Fetzer F, Sommer M, Weber R, et al. Reduction of pores by means of laser beam oscillation during remote welding of Al-Mg-Si [J]. Optics and Lasers in Engineering, 2018, 108: 68-77.
- [114] Rubben K, Mohrbacher H, Leirman E. Advantages of using an oscillating laser beam for the production of tailored blanks[J]. Proceedings of SPIE, 1997, 3097: 228-241.
- [115] 周立涛, 王旭友, 王威, 等. 激光扫描焊接工艺对铝合金焊接气孔率的影响[J]. 焊接学报, 2014, 35(10): 65-68, 72, 116.
- Zhou L T, Wang X Y, Wang W, et al. Effects of laser scanning welding process on porosity rate of aluminum alloy[J]. Transactions of the China Welding Institution, 2014, 35(10): 65-68, 72, 116.
- [116] Liu T T, Mu Z Y, Hu R Z, et al. Sinusoidal oscillating laser welding of 7075 aluminum alloy: hydrodynamics, porosity formation and optimization[J]. International Journal of Heat and Mass Transfer, 2019, 140: 346-358.
- [117] Chen G Y, Wang B, Mao S, et al. Research on the “∞”-shaped laser scanning welding process for aluminum alloy[J]. Optics & Laser Technology, 2019, 115: 32-41.
- [118] 杨蓉. 激光扫描焊接工艺在铝合金焊接中的应用研究[J]. 现代制造技术与装备, 2017(2): 106, 108.
- Yang R. Application of laser scanning welding process in aluminum alloy welding[J]. Modern Manufacturing Technology and Equipment, 2017(2): 106, 108.
- [119] Zhang C, Yu Y, Chen C, et al. Suppressing porosity of a laser keyhole welded Al-6Mg alloy via beam oscillation[J]. Journal of Materials Processing Technology, 2020, 278: 116382.
- [120] 温鹏, 栗忠秀, 张松, 等. 摆动光纤激光-CMT 复合焊接 6A01-T5 铝合金型材接头的气孔特征及组织性能研究[J]. 中国激光, 2020, 47(8): 0802003.
- Wen P, Li Z X, Zhang S, et al. Investigation on porosity, microstructures and performances of 6A01-T5 aluminum alloy joint by oscillating fiber laser-CMT hybrid welding[J]. Chinese Journal of Lasers, 2020, 47(8): 0802003.
- [121] 蔡创, 谢佳, 刘致杰, 等. 铝合金摆动激光-MIG 复合焊接特性及气孔控制[J]. 中国激光, 2021, 48(18): 1802002.
- Cai C, Xie J, Liu Z J, et al. Welding characteristics and porosity control of weaving laser-MIG hybrid welding of aluminum alloys [J]. Chinese Journal of Lasers, 2021, 48(18): 1802002.
- [122] Wang L, Gao M, Hao Z Q. A pathway to mitigate macrosegregation of laser-arc hybrid Al-Si welds through beam oscillation[J]. International Journal of Heat and Mass Transfer, 2020, 151: 119467.
- [123] Li Y, Zhao Y Q, Zhou X D, et al. Effect of droplet transition on the dynamic behavior of the keyhole during 6061 aluminum alloy laser-MIG hybrid welding[J]. The International Journal of Advanced Manufacturing Technology, 2022, 119(1): 897-909.
- [124] Wu D S, Ishida K, Tashiro S, et al. Dynamic keyhole behaviors and element mixing in paraxial hybrid plasma-MIG welding with a gap [J]. International Journal of Heat and Mass Transfer, 2023, 200: 123511.
- [125] Ascarì A, Fortunato A, Orazi L, et al. The influence of process parameters on porosity formation in hybrid LASER-GMA welding of AA6082 aluminum alloy[J]. Optics & Laser Technology, 2012, 44(5): 1485-1490.
- [126] Chen X Y, Yu G, He X L, et al. Effect of droplet impact on molten pool dynamics in hybrid laser-MIG welding of aluminum alloy[J]. The International Journal of Advanced Manufacturing Technology, 2018, 96(1): 209-222.
- [127] 张羽昊, 陈辉, 杨策, 等. 激光功率对铝合金激光-MIG 复合焊熔滴过渡行为及飞溅的影响[J]. 激光与光电子学进展, 2022, 59(17): 1714005.
- Zhang Y H, Chen H, Yang C, et al. Influence of laser power on droplet transfer behavior and spatter in laser-MIG hybrid welding of aluminum alloy[J]. Laser & Optoelectronics Progress, 2022, 59(17): 1714005.
- [128] 徐锴, 武鹏博, 李琳琳, 等. 铝合金激光-多股绞合焊丝 MIG 复合焊接头组织与性能分析[J]. 焊接学报, 2022, 43(11): 43-49, 165.
- Xu K, Wu P B, Li L L, et al. Microstructure and performance analysis of laser-MIG hybrid welding joints of aluminum alloy with multi-stranded wire[J]. Transactions of the China Welding Institution, 2022, 43(11): 43-49, 165.
- [129] 李巧艳, 赵昕, 辛志彬, 等. 6082 铝合金激光-MIG 复合焊接工艺及接头组织性能[J]. 应用激光, 2021, 41(6): 1168-1177.
- Li Q Y, Zhao X, Xin Z B, et al. Welding process and mechanical properties of laser-MIG hybrid welding for 6082 aluminum alloy[J]. Applied Laser, 2021, 41(6): 1168-1177.
- [130] 刘婷, 赵艳秋, 周旭东, 等. 能量配比系数对铝合金激光-MIG 复合焊接气孔的影响[J]. 中国激光, 2020, 47(11): 1102004.
- Liu T, Zhao Y Q, Zhou X D, et al. Effect of energy ratio coefficient on pore during aluminum alloy laser-MIG hybrid welding [J]. Chinese Journal of Lasers, 2020, 47(11): 1102004.
- [131] Zhang C, Gao M, Wang D Z, et al. Relationship between pool characteristic and weld porosity in laser arc hybrid welding of AA6082 aluminum alloy[J]. Journal of Materials Processing Technology, 2017, 240: 217-222.
- [132] Wang J F, Sun Q J, Feng J C, et al. Characteristics of welding and arc pressure in TIG narrow gap welding using novel magnetic arc oscillation[J]. The International Journal of Advanced Manufacturing Technology, 2017, 90(1): 413-420.
- [133] Tse H C, Man H C, Yue T M. Effect of magnetic field on plasma control during CO₂ laser welding[J]. Optics & Laser Technology, 1999, 31(5): 363-368.
- [134] Li M, Xu J J, Huang Y, et al. Improving keyhole stability by external magnetic field in full penetration laser welding[J]. JOM, 2018, 70(7): 1261-1266.
- [135] Chen J C, Wei Y H, Zhan X H, et al. Influence of magnetic field orientation on molten pool dynamics during magnet-assisted laser butt welding of thick aluminum alloy plates[J]. Optics & Laser Technology, 2018, 104: 148-158.
- [136] Zhu Z W, Ma X Q, Wang C M, et al. Modification of droplet morphology and arc oscillation by magnetic field in laser-MIG hybrid welding[J]. Optics and Lasers in Engineering, 2020, 131: 106138.
- [137] Liu F Y, Tan C W, Wu L J, et al. Influence of waveforms on Laser-MIG hybrid welding characteristics of 5052 aluminum alloy assisted by magnetic field[J]. Optics & Laser Technology, 2020, 132: 106508.
- [138] Deng J W, Chen C, Liu X C, et al. A high-strength heat-resistant Al-5.7Ni eutectic alloy with spherical Al₃Ni nano-particles by selective laser melting[J]. Scripta Materialia, 2021, 203: 114034.
- [139] Farkoosh A R, Chen X G, Pekguleryuz M. Dispersoid strengthening of a high temperature Al-Si-Cu-Mg alloy via Mo addition[J]. Materials Science and Engineering: A, 2015, 620: 181-189.

- [140] Khodabakhshi F, Nosko M, Gerlich A P. Effects of graphene nano-platelets (GNPs) on the microstructural characteristics and textural development of an Al-Mg alloy during friction-stir processing[J]. Surface and Coatings Technology, 2018, 335: 288-305.
- [141] Ye T K, Xu Y X, Ren J. Effects of SiC particle size on mechanical properties of SiC particle reinforced aluminum metal matrix composite[J]. Materials Science and Engineering: A, 2019, 753: 146-155.
- [142] Poovazhagan L, Kalaichelvan K, Rajadurai A, et al. Characterization of hybrid silicon carbide and boron carbide nanoparticles-reinforced aluminum alloy composites[J]. Procedia Engineering, 2013, 64: 681-689.
- [143] Mazahery A, Ostadshabani M. Investigation on mechanical properties of nano-Al₂O₃-reinforced aluminum matrix composites [J]. Journal of Composite Materials, 2011, 45(24): 2579-2586.
- [144] Metlitskii V A. Flux-cored wires for arc welding and surfacing of cast iron[J]. Welding International, 2008, 22(11): 796-800.
- [145] Senthilkumar B, Kannan T, Madesh R. Optimization of flux-cored arc welding process parameters by using genetic algorithm[J]. The International Journal of Advanced Manufacturing Technology, 2017, 93(1): 35-41.
- [146] 朱宝华, 李小婷, 丁凯强. 半导体-光纤激光复合焊接铝合金研究[J]. 应用激光, 2018, 38(4): 587-590.
- Zhu B H, Li X T, Ding K Q. Research on hybrid diode-fiber laser welding for aluminum alloy[J]. Applied Laser, 2018, 38(4): 587-590.
- [147] Zhao Y Q, Li X, Liu Z Q, et al. Stability enhancement of molten pool and keyhole for 2195 Al-Li alloy using fiber-diode laser hybrid welding[J]. Journal of Manufacturing Processes, 2023, 85: 724-741.
- [148] Yang H, Tang X H, Hu C, et al. Study on laser welding of copper material by hybrid light source of blue diode laser and fiber laser[J]. Journal of Laser Applications, 2021, 33(3): 032018.
- [149] Wu D S, Sun J H, Li Z G, et al. Molten pool behaviors and energy absorption in coaxial hybrid blue-IR lasers welding of a copper material[J]. International Journal of Thermal Sciences, 2023, 184: 107945.

Review of Laser-Arc Hybrid Welding Process of Aluminum Alloys for New Energy Vehicles (Invited)

Wang Xiaonan^{1,2*}, Chen Xiaming^{1,2}, Huan Pengcheng³, Li Xiang⁴, Dong Qipeng^{1,2}, Luo Shuncun^{1,2}, Nagaumi Hiromi^{1,2}

¹School of Iron and Steel, Soochow University, Suzhou 215021, Jiangsu, China;

²Jiangsu Engineering Research Center for Green Preparation and Resource Recycling of New Energy Vehicles Metal, Suzhou 215021, Jiangsu, China;

³State Key Laboratory of Rolling and Automation, Northeastern University, Shenyang 110819, Liaoning, China;

⁴Ruike Fiber Laser Technology Co., Ltd., Wuxi 214000, Jiangsu, China

Abstract

Significance The development of new energy vehicles is the effective way for China to transition from a large automobile country to an automobile power; this is also a strategic initiative to address climate change and promote green development. As important materials for manufacturing new energy vehicles, the excellent mechanical properties of automotive aluminum alloys have brought new challenges during the subsequent welding processes. The original fine grains and nanoprecipitates of the automotive aluminum alloy are destroyed by the welding heat source, producing noticeable softening in the weld seam and heat-affected zone. Consequently, the mechanical properties of traditional arc-welded joints are inferior to the requirements of industrialization. High-quality and efficient welding of automobile aluminum alloys is a development trend, and traditional welding processes struggle to satisfy this demand.

The high-power-density fusion welding process, that is, the laser welding process with low heat input, is used to shorten the softening zone and reduce the adverse effects of the heat source on the substrate plates. Moreover, it also significantly improves welding efficiency because of its high power density. However, as a high inversion material, the laser absorption of aluminum alloys is less than 5%, leading to enormous energy wastage and danger. Meanwhile, the fine spot (diameter of 0.2–0.6 mm) indicates the poor bridging ability of the laser welding process, and the burning loss produces a weld seam with a poor forming quality and high softening degree. Thus, a laser-arc hybrid welding process is used to weld the aluminum alloy. In the laser-arc hybrid welding process, the laser beam and arc interact in a common weld pool, and their synergic effect increases laser absorption and bridging ability. Moreover, wire filling compensates for the burning loss, thereby improving the forming quality and mechanical properties of the weld seam. At the beginning of the 21st century, a laser-arc hybrid welding process was applied to car structure manufacturing. Since then, researchers from China, Italy, and Canada have focused on regulating the microstructure and mechanical properties of laser-arc hybrid welded joints. Owing to the substantial reduction in the price of laser machines, laser-arc hybrid welding of aluminum alloys has received more attention in the past three years.

Process Automobile aluminum alloys are divided into two categories: heat-treatable aluminum alloys [Al-Mg-Si(Cu)] and Al-Zn-Mg

(-Cu)] and non-heat-treatable aluminum alloys [Al-Mg(-Mn)]. Considering their characteristics, typical welding defects such as softening, pores, and hot cracking are summarized in Fig. 4, and the softening mechanisms of the heat-affected zone and weld seam are analyzed and summarized in Figs. 5 and 6. The regulatory mechanisms of welded joints using the laser-cold metal transfer (CMT) hybrid welding process and welding seam alloying (solute elements, refined grain elements, and nanometallic intermetallic compounds with high melting points) are summarized in Figs. 8 and 9. The formation mechanism of typical pores in laser-arc hybrid weld is summarized in Fig. 12. To suppress keyhole-induced pores, a scanning laser-arc hybrid welding process is used to improve keyhole stability. The suppression mechanism is illustrated in Fig. 14. Other methods for suppressing keyhole collapse including process parameter optimization, droplet transfer behavior regulation, and external field assistance are also analyzed in this study. Finally, this study summarizes the current problems in the laser-arc hybrid welding process of aluminum alloys and proposes future development trends.

Conclusions and Prospects The laser-arc hybrid welding process has many advantages in suppressing welding defects and improving the welding coefficient of automobile aluminum alloys. Based on the softening mechanism, the softening degree of the welded joints is effectively decreased by innovation in the welding process and optimization of the alloying elements. However, commercial welding wires cannot be used for fabricating weld seams with excellent mechanical properties. Enhancing weld seams by welding seam alloying requires extensive research and exploration. Meanwhile, flux-cored welding wires that can be flexibly composition-designed and short-produced are more suitable for the development of new ground filling materials. Recently, new hybrid laser sources such as hybrid diode-fiber lasers, hybrid blue-light diode-fiber lasers, and core-diameter ring light spots have been used to improve the weld formation of automobile aluminum alloys. Thus, the effect of new laser technology on welding defects, particularly pores in laser-arc weld seams, still requires extensive research and exploration.

Key words laser technique; laser-arc hybrid welding; aluminum alloys; softening; pore; mechanical property